

UNIVERSITY OF CALIFORNIA
Los Angeles

The Effect of Dissolved Oxygen Probe Lag
Upon Oxygen Transfer Parameter Estimation


A thesis submitted in partial satisfaction of the
requirements for the degree Master of Science
in Engineering

by

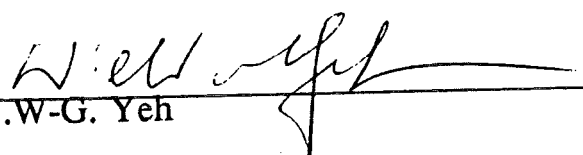
Theodore L. Philichi

1987


The thesis of Theodore L. Philichi is approved.



J.B. Neethling



W.W-G. Yeh



Michael K. Stenstrom, Committee Chair

University of California, Los Angeles

1987

TABLE OF CONTENTS

	Page
LIST OF FIGURES.....	iv
LIST OF TABLES	vi
ACKNOWLEDGMENT	vii
ABSTRACT.....	viii
I. INTRODUCTION	1
II. LITERATURE REVIEW	6
A. The Nonsteady-State Clean Water Test	6
B. The Polarographic Oxygen Probe.....	10
C. Nonsteady-State Probe Response	24
D. Summary.....	28
III. RESEARCH PROCEDURE	29
A. Experimental Procedures.....	29
1. Apparatus.....	29
2. Test Initialization Procedure	31
3. The Probe Lag Test	34
4. The Clean Water Test.....	38
B. Probe Simulation	44
VI. EXPERIMENTAL RESULTS.....	46
V. CONCLUSIONS	59
VI. REFERENCES.....	61

LIST OF FIGURES

	Page
Figure 1. Variations in Clean Water Test Data (After Gilbert et al. (1978))	3
Figure 2. Typical Nonsteady-State Probe Response (After Aiba (1973))	4
Figure 3. Typical Change in Dissolved Oxygen During Aeration	9
Figure 4. The Logarithmic Procedure	11
Figure 5. Typical Current Output Curve (After Barns (1979))	17
Figure 6. Temperature Effect on Current Output (After Hitchman (1979))	19
Figure 7. Probe Diffusion Field (After Aiba (1973))	21
Figure 8. Probe Diffusion Layers (After Hitchman (1978))	25
Figure 9. Nonsteady-State Probe Response (After Aiba and Huang (1969))	26
Figure 10. Basic Test Apparatus	30
Figure 11. Test Apparatus Diffused Air System	32
Figure 12. Lag Test Procedure	36
Figure 13. Time Constant Calculation	39
Figure 14. Time Constant Calculation	40

Figure 15. Typical Log-Log Response for 2nd Order Time Constant	41
Figure 16. Clean Water Test Results for Two Different Types of Membranes	43
Figure 17. Ratio of Estimated $K_L a$'s to True $K_L a$'s	58
Figure 18. Ratio of Estimated $K_L a$ to True $K_L a$	55
Figure 19. Residuals for a Fast Response Probe Versus Time, Truncated and Untruncated	57
Figure 20. Residuals for a Medium Response Probe Versus Time, Truncated and Untruncated	58

LIST OF TABLES

	Page
Table 1 Summary of Experimental Results.....	47
Table 2 Simulation Results.....	52

ACKNOWLEDGMENT

I wish to express my utmost appreciation to my graduate advisor, Dr. Michael K. Stenstrom for his unwavering support, patience and friendship throughout graduate study; and to members of the Masters committee, Professors William Y-G. Yeh and J.B. Neethling.

I also wish to thank my family for their patience and support.

ABSTRACT OF THE THESIS

The Effect of Dissolved Oxygen Probe Lag Upon Oxygen Transfer Parameter Estimation

by

Theodore L. Philichi

Master of Science in Engineering

University of California, Los Angeles, 1987

Professor Michael K. Stenstrom, Chair

Oxygen transfer is one of the most energy consumptive aspects of aerobic biological wastewater treatment. In order to better define oxygen transfer the American Society of Civil Engineers developed a standard procedure for testing oxygen transfer. This standard recommends that dissolved oxygen concentration be measured using polarographic sensors, commonly called dissolved oxygen probes or electrodes.

Dissolved oxygen probes are imperfect and require a finite length of time to respond to a change in dissolved oxygen concentration. This time delay can influence the results of the standard oxygen testing procedure.

To determine the magnitude of this potential effect a series of experiments were performed, and a mathematical model of the probe and standard test were developed. The dissolved oxygen probes were modeled as linear first-order systems, with a time constant, τ . A test procedure was developed to experimentally estimate time constants for a popular brand of probe with several membrane configurations. Next, these modified probes with known time constants were used to measure oxygen transfer in a laboratory scale test vessel. The magnitude of the mass transfer coefficient estimated from probes with significant time lag was compared to fast probes.

It was shown that the probe-lag induced error in estimating the mass transfer coefficient ($K_L a$) was less than 1% when the product of probe time constant and $K_L a$ were less than 0.02. If the concentration versus time data are truncated at 20% of the final equilibrium value, probe lag induced error is much less, indicating that higher values of $K_L a$ or slower probes can be used without increasing the measured error in $K_L a$. The product of $K_L a$ and τ increase to 0.05 without introducing more than 1% error in $K_L a$.

I. INTRODUCTION

Aeration systems in conventional activated sludge treatment plants are usually the most expensive aspect of plant operations (Hitchman, 1978), often comprising 60% to 80% of the plant's energy requirements (Stenstrom, et al. 1984). Accordingly, a great deal of effort has been placed on the evaluation of aeration systems, to ensure their performance at minimum cost.

Throughout the industry there appears to be a consensus that the clean water nonsteady-state aeration test is the best method for performing the required evaluations and compliance tests. The popularity of this method is well documented in the literature (Ewing, et al. 1977; Brown and Bailod, 1982). An industry-wide effort lead to the publication of a Clean Water Test Standard (ASCE, 1984). Using the Standard, manufacturers, owners, and researchers can measure uniform and consistent Standard Oxygen Transfer Rates (SOTR's) and Standard Aeration Rates (SAE's). The procedure requires that dissolved oxygen (DO) concentration measurements be taken over an extended period in the tanks being tested. These measurements are taken with respect to time as the water is aerated from measurements near zero DO concentration to close to saturation.

A polarographic dissolved oxygen probe is commonly used to determine the dissolved oxygen during the test. While this is a convenient method for obtaining these values, there has been some concern expressed in the literature as to whether the probe's response time delay affects test results. (Aiba, 1973; Gilbert and Chen, 1976; Stenstrom, 1978). Gilbert and Chen showed the effects of this delay through their determinations of the dissolved oxygen with respect to time as a function of the probe's time constant, as shown in Figure 1.

Aiba (1973) empirically tested the probe lag, creating the chronological output shown in Figure 2, as the probe was first exposed to oxygen enriched waters, and then exposed oxygen depleted water. Gilbert and Chen noted that it takes about 30 seconds for a probe to reach 99% of the actual steady-state dissolved oxygen value. Aiba noted a general time of between 10 and 100 seconds for the probe to achieve 90% of the steady-state value. While these time periods are only generalized values found in the literature and varying with each instrument, they indicate the approximate response time of DO probes traditionally used in oxygen transfer testing.

Both Gilbert (1976) and Stenstrom (1978), have quantified the magnitude of probe-lag induced error. They both have observed that the error created by probe lag is negligible if probe lag is much less than the reciprocal of $K_L a$. Stenstrom discussed this by referencing a variable for the probe time constant,

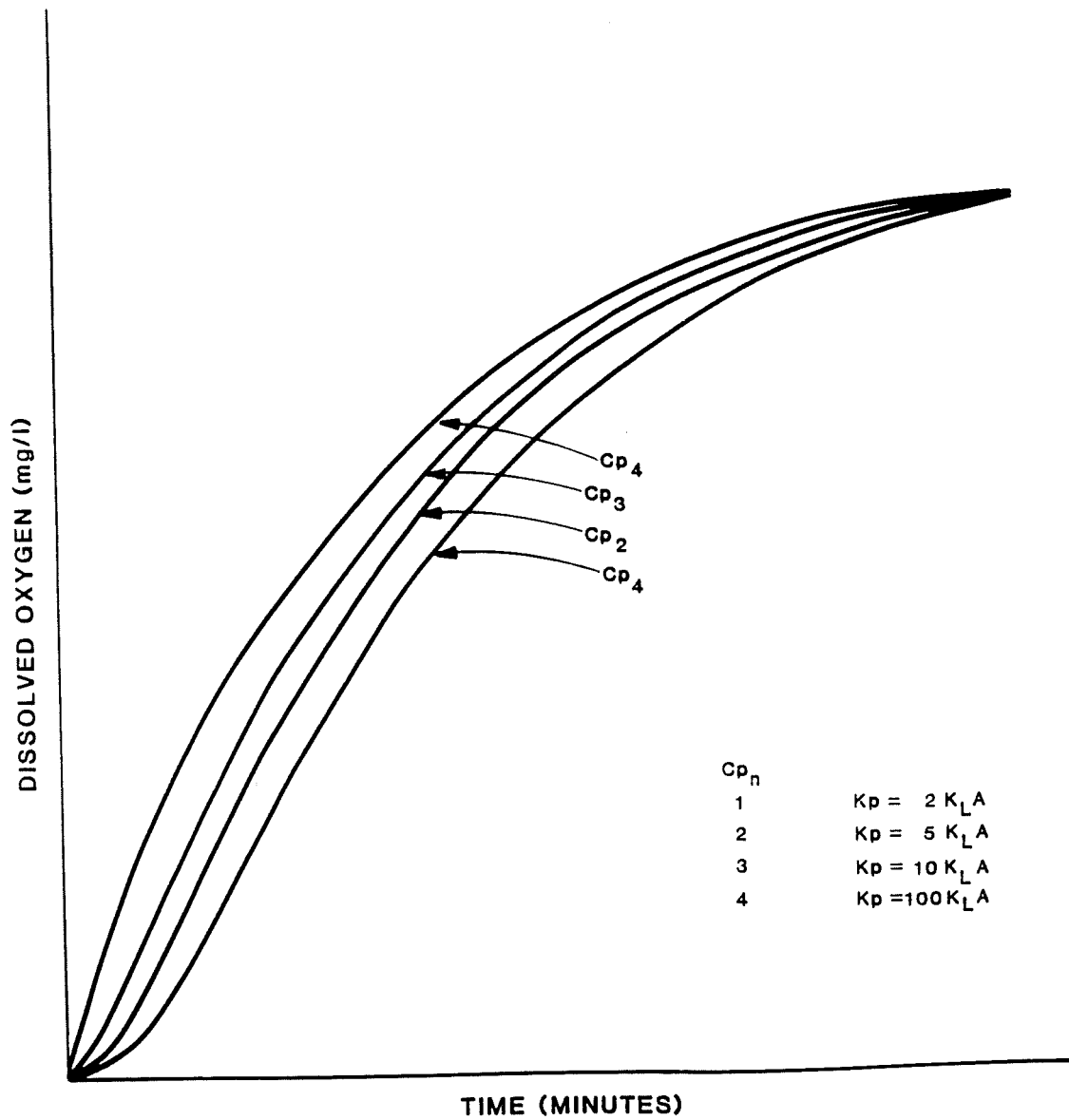


Figure 1. Variations in Clean Water Test Data
(After Gilbert et al. (1978))

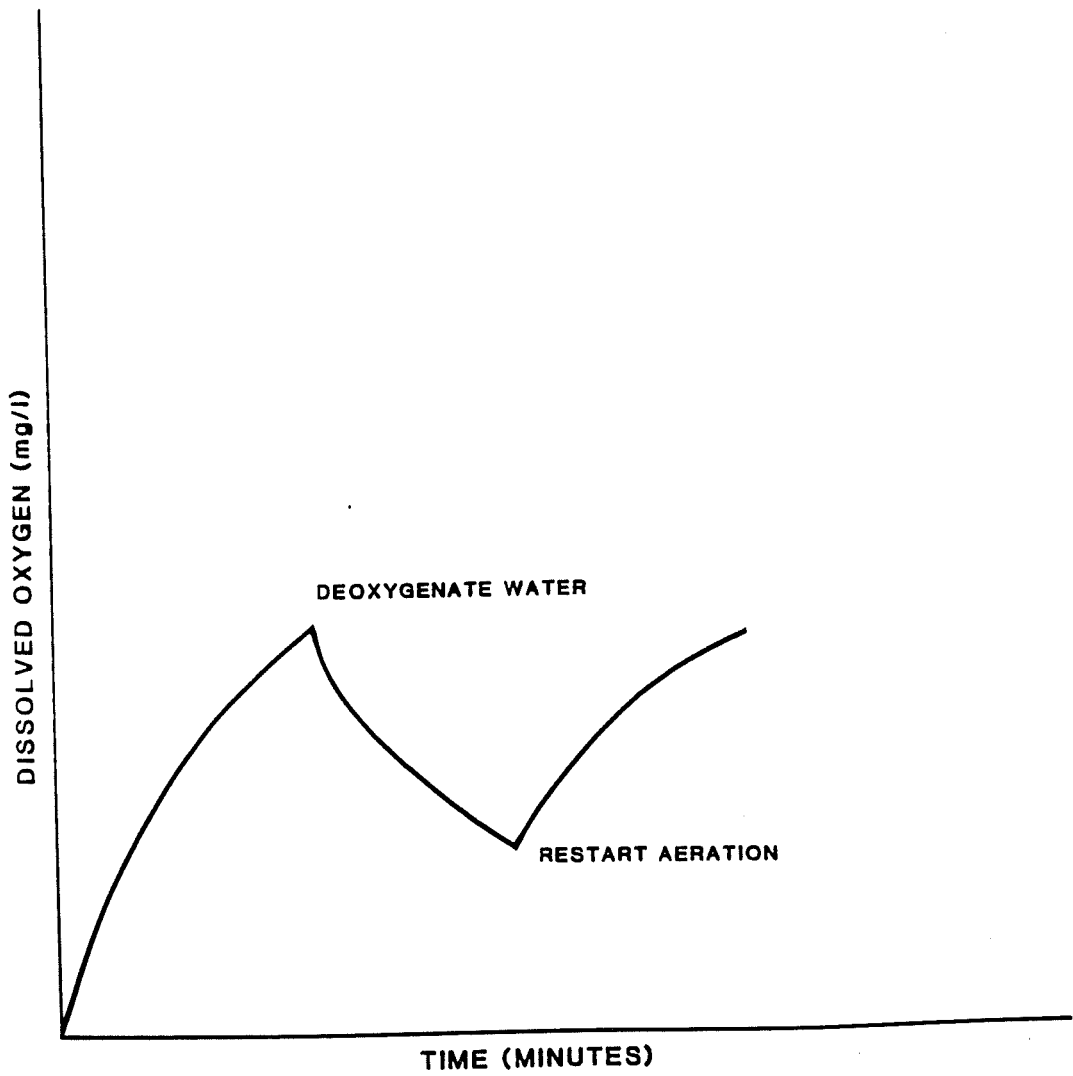


Figure 2. Typical Nonsteady-State Probe Response (After Aiba (1973))

τ . The reciprocal of $K_L a$ can also be thought of as a time constant, corresponding to the aeration system/tank time constant. His results have been included in the ASCE Standard, 1984.

The objective of this research is to quantify the magnitude of probe lag induced error on $K_L a$ estimation in the clean water nonsteady-state test. A review of the relevant literature is provided. The results of a series of laboratory experiments, supported by computer simulations, is also provided.

II. LITERATURE REVIEW

To become familiar with the causes and effects of probe-lag the literature has been reviewed. The clean water test procedure will be briefly explained, followed by a description of the polarographic oxygen electrode, and the nonsteady-state probe response.

A. The Nonsteady-State Clean Water Test

The nonsteady-state test clean water (tap water) is a method to evaluate an aeration system as clean water is aerated from a dissolved oxygen concentration of near zero to a concentration close to its equilibrium value. The test begins by deoxygenating the water. This is performed by adding sodium sulfite and cobalt chloride catalyst to the water being aerated. Alternatively, in laboratory studies, nitrogen can be used to strip the dissolved oxygen. After the dissolved oxygen decreases to 0.5 mg/L or less, aeration is begun and the dissolved oxygen concentration is measured over time. For large basins, multiple sampling locations are used. Typically a minimum of 21 dissolved oxygen values are taken during the test (ASCE, 1984). The test is continued until the dissolved oxygen concentration exceeds 96% of the equilibrium concentration.

A nonlinear exponential parameter estimation procedure is used to analyze the DO concentration versus time data. Estimates for the mass transfer

coefficient, $K_L a$, equilibrium dissolved oxygen concentration, C_∞^* , and initial DO concentration, C_o are obtained. These values are then used to determine the oxygen transfer rates and the efficiency of the system.

The nonsteady-state clean water oxygen transfer test is well understood and is based upon the two film theory of Lewis and Whitman, (1924). Campbell, Ball, and O'Brien, (1976) and Brown and Bailod, (1982) have reviewed the test procedures and mathematical development in detail, and therefore, only a brief summary is provided here.

The change in the dissolved oxygen in water with respect to time can be described as follows:

$$\frac{dC}{dt} = K_L a (C_\infty^* - C) \quad (1)$$

$K_L a$ = apparent mass transfer coefficient

C_∞^* = equilibrium dissolved oxygen concentration, attained as the time approaches infinity.

C = bulk concentration at time, t .

t = elapsed time.

This relationship, expressed in Equation (1), can be utilized in three ways for the evaluation of the nonsteady-state test data. The three parameter estimation techniques are as based upon the following forms of Equation (1):

Differential form:

$$\frac{dC}{dt} = K_L a (C_\infty^* - C) \quad (2)$$

Logarithmic form:

$$\ln \frac{C_\infty^* - C}{C_\infty^* - C_0} = -K_L a t \quad (3)$$

Exponential form:

$$C = C_{in}^* - (C_\infty^* - C_0) \exp(K_L a^* t) \quad (4)$$

Both the exponential and the logarithmic forms are recommended by Brown and Bailod (1982), while the ASCE Standard accepts only the exponential form. With the exponential method, the parameters, $K_L a$, C_∞^* , and C_0 , are estimated using a nonlinear least squares fit procedure. Typical results of this procedure are shown in Figure 3.

The logarithmic forms can be utilized in two ways for the parameter estimation. These are the best-fit log deficit method and the log difference method. With the best fit method, values of $K_L a$ are determined using a linear least squares fit procedure while iteratively estimating the value of C_∞^* to make the calculated values most closely approximate the data, e.g., minimizing the sum

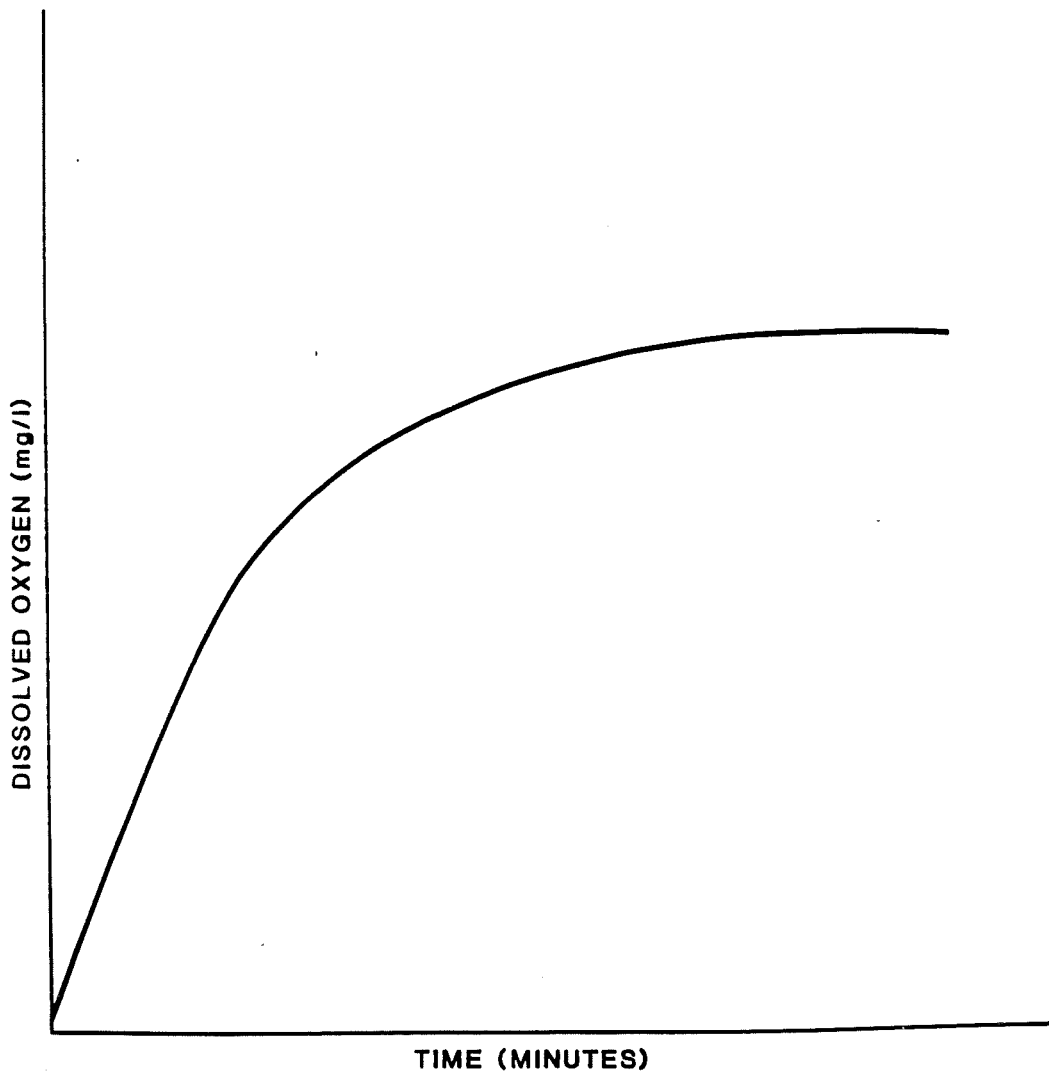


Figure 3. Typical Change in Dissolved Oxygen During Aeration

of squares error. When using the log difference method, one must use *a priori* estimates of C_{∞}^* , and calculate $K_L a$ using linear least squares. This last method is very popular but is not included in the ASCE Standard, since biased results are usually obtained. The logarithmic procedure is shown in Figure 4.

There are errors associated with the use of both methods. Boyle, Berthouex, and Rooney (1974) discussed these errors caused by poor estimations of C_{∞}^* when using the log difference. Brown and Bailod (1982) explained that when using exponential form, the error due to the measured concentration values, C , are greatest at the beginning of the test. For the differential case, they note the associated error with the deficit, $C_{\infty}^* - C$, increases as the deficit becomes larger. Gilbert and Chen (1976) and Stenstrom (1978) have postulated ways in which probe-lag induced errors affect these procedures.

B. The Polarographic Oxygen Probe

When performing the nonsteady-state clean water test according to the ASCE Standard, the dissolved oxygen concentration can be measured by either modified Winkler analysis using pumped samples, or in-situ dissolved oxygen probes. When using the Winkler test, water is usually pumped from several points in the tank to sample bottles located at a central point. Samples are collected at predetermined time intervals. The samples are immediately stabilized and are titrated at the conclusion of the test. The modified Winkler procedure is

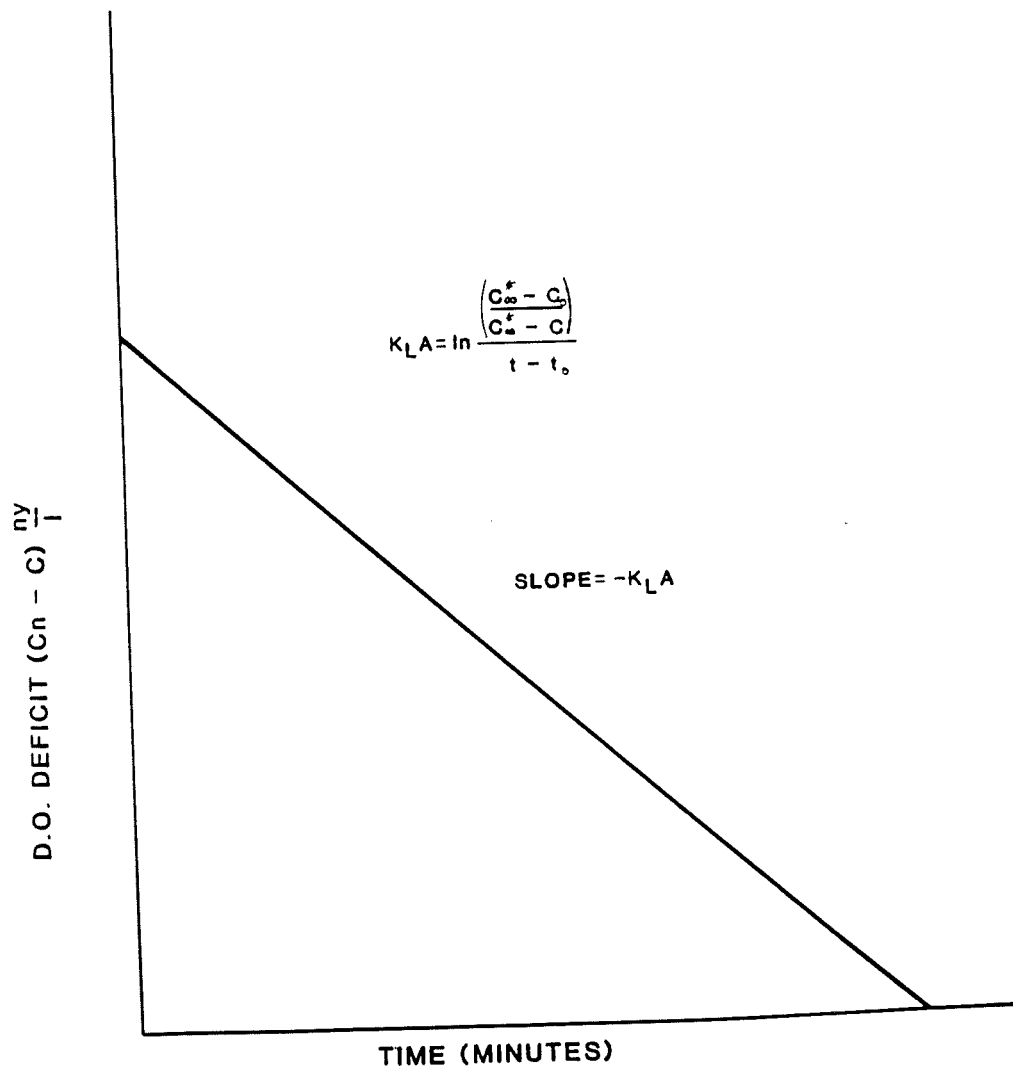


Figure 4. The Logarithmic Procedure

described in *Standard Methods* (1985).

With the in-situ probe method, polarographic oxygen probes, with continuous signal read out, are placed at numerous representative points throughout the tanks. The dissolved oxygen values are determined by periodically reading the probe's indicator, or by attached, continuous recorders.

Most investigators believe that the probe method is considerably easier to work with than the Winkler method. The simplicity and accuracy of probes has made this the method of choice throughout the industry (Reynolds, 1969).

Dissolved oxygen probes are currently used extensively throughout the water treatment industry. Reynolds (1969), compared a membrane covered polarographic dissolved oxygen probe with the Winkler method for steady-state dissolved oxygen measurements and found practically the same results. Unfortunately, published nonsteady-state comparison of the two methods are somewhat scarce. Ewing, Redmon and Wren (1977), compared the final $K_L a$ results obtained by the two methods. They found slight differences, but did not place great significance upon their conclusions.

The dissolved oxygen probe is an instrument which transmits and displays an electrical signal which is dependent on the dissolved oxygen being measured, through the use of a galvanic cell. This cell consists of an anode, a

described in *Standard Methods* (1985).

With the in-situ probe method, polarographic oxygen probes, with continuous signal read out, are placed at numerous representative points throughout the tanks. The dissolved oxygen values are determined by periodically reading the probe's indicator, or by attached, continuous recorders.

Most investigators believe that the probe method is considerably easier to work with than the Winkler method. The simplicity and accuracy of probes has made this the method of choice throughout the industry (Reynolds, 1969).

Dissolved oxygen probes are currently used extensively throughout the water treatment industry. Reynolds (1969), compared a membrane covered polarographic dissolved oxygen probe with the Winkler method for steady-state dissolved oxygen measurements and found practically the same results. Unfortunately, published nonsteady-state comparison of the two methods are somewhat scarce. Ewing, Redmon and Wren (1977), compared the final $K_L a$ results obtained by the two methods. They found slight differences, but did not place great significance upon their conclusions.

The dissolved oxygen probe is an instrument which transmits and displays an electrical signal which is dependent on the dissolved oxygen being measured, through the use of a galvanic cell. This cell consists of an anode, a

cathode, and an electrolyte, creating an oxidation-reduction reaction where the rate is dependent on the amount of available oxygen.

The electrical current which the reaction provides is quantitatively a function of the amount of oxygen reacting at the cathode's surface. This is described by Faraday's law as follows:

$$i = FnAN \quad (5)$$

where

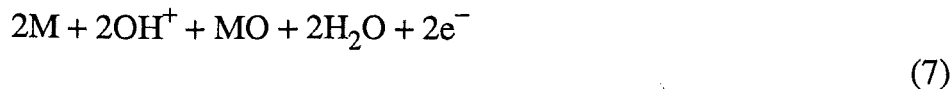
- i = steady-state current from the reaction of the cell
- F = Faraday's constant (96,500 cal/g equiv)
- n = number of electrons required for the oxidation reduction
- A = effective area of the cathodes surface
- N = oxygen flux entering the probe, (Aiba and Huang (1969))

The basic chemical reactions which take place within the probe have been explained by Mancy and Westgarth (1962), and Hitchman (1978), as follows:

Cathodic reaction:



Anodic reaction:



where M is the metal used for the anode.

As can be seen, the cathode is the site where the reduction reaction takes place, while the anode is the site of the oxidation reaction. The main purpose of the electrolyte is to furnish a medium for ionic conduction between the anode and the cathode and to furnish ions for the half cell anodic reaction, (Barns, 1979).

This galvanic principle can be used in a number of ways to measure dissolved oxygen. Materials can be used for the anode and cathode with relative potential differences great enough to force the reaction to proceed as the oxygen becomes available. This type of system has been referred to as a "Galvanic Detector" (Hitchman, 1978).

The other more common method, referred to in the literature as the "polarographic" or "voltammetric" detector, uses an applied voltage between the electrodes to create this potential difference (Hitchman, 1978). This method allows the operating voltage to be specified and higher accuracy can be achieved.

The polarographic concept was first introduced in 1922 by Heyrousky at Charles University in Prague (Reynolds, 1969). By 1924 the dropping mercury electrode or DME method had been utilized for dissolved oxygen measurement, Morgan and Bewtra (1962). This method uses a small charged mercury drop falling through the test solution as the cathode and the relatively large underlying reservoir of mercury at the bottom as the anode. An electrolyte was injected directly into the test solution. As reported by Morgan and Bewtra (1962), this method was able to produce accuracies within 7% of the Winkler method when measuring dissolved oxygen. This DME method was also discussed by Rand and Heukelekian (1951). The rotating platinum method is also discussed in the literature (Mancy, Okun and Reilley, 1961).

As polarographic technology progressed, it was discovered that exposing the cathode and the anode directly to the sample being measured had deleterious effects on the accuracy of the results. This was due to two causes: 1) the surface active impurities within the sample were reacting with the electrodes and said to be "poisoning" them, and 2) the electrolyte was allowed to change with time. Both of these cause the steady-state results to vary (Hitchman, 1978). Other failure mechanisms have been discussed in the literature and include: 1) contamination of the cathode environment, 2) shifts in the equilibrium potential, and 3) change in the diffusion field (Barnes, 1979).

Clark (1957) introduced a method which revolutionized polarographic dissolved oxygen measurement and solved the aforementioned deficiencies. While working on a measurement method for blood oxygen, Clark designed and patented a cell with both the anode, cathode, and electrolyte separated from the sample solution by an oxygen permeable membrane. This method is the basis for most polarographic dissolved oxygen measurement today (Clark, 1957).

Membrane materials are listed in the literature (Hitchman, 1979). They include polyethylene, natural rubber, silicone rubber, PVC, polyethylene (PTFE), and fluorinated plastics (FED). The principle criteria for these materials include: 1) availability, 2) high strength, 3) constant oxygen permeability, and 4) a low degree of crystallinity.

The materials used for the anodes and cathodes vary from probe to probe. Typically the anode is composed of a base metal like zinc, lead, or cadmium, and the cathode is composed of a noble metal which can be used for reduction. The YSI (1977) probes used in this laboratory contain a silver anode and a gold cathode.

A typical current output curve for a polarographic dissolved oxygen probe is shown in Figure 5 (Barnes, 1979). One can observe that there exists a plateau region on the graph where the current is practically constant. This has

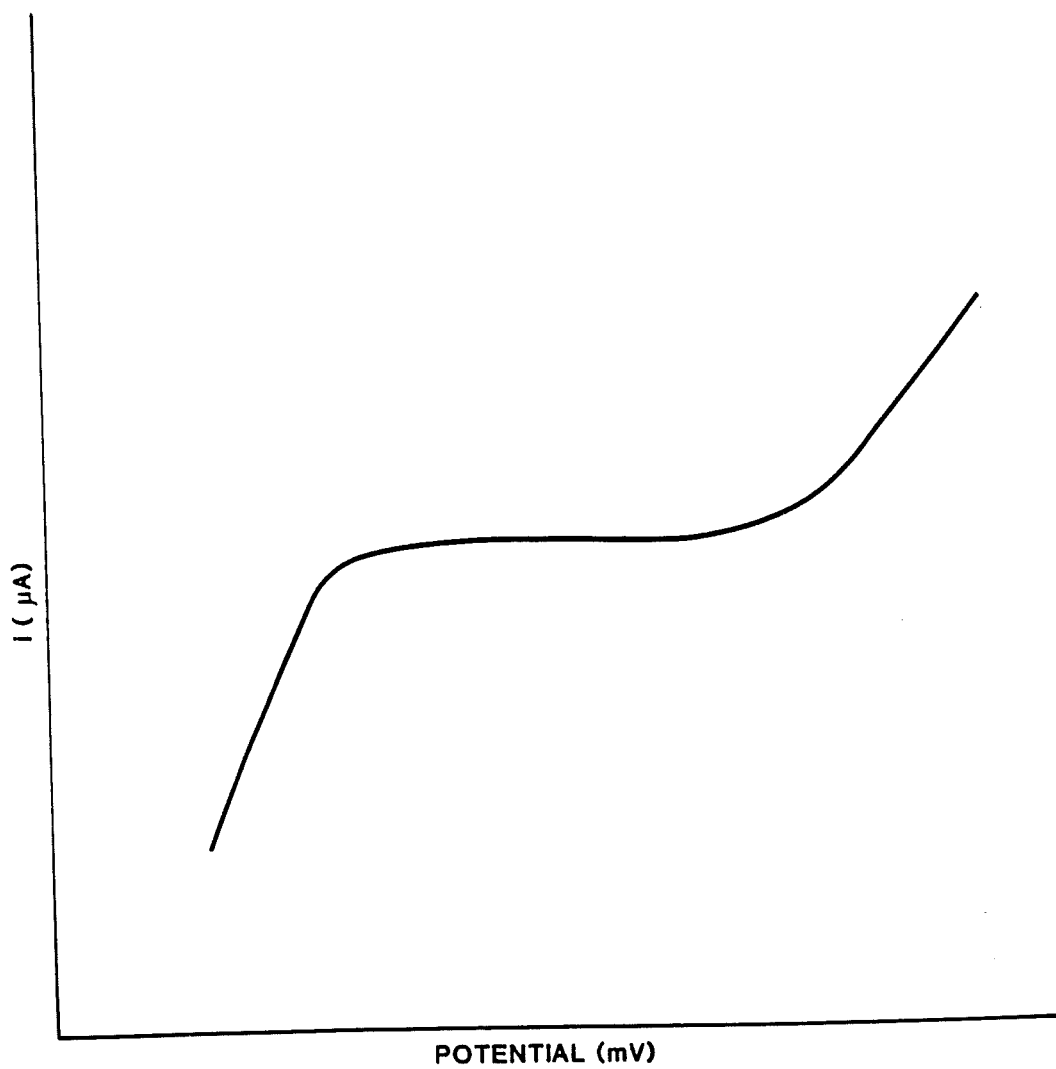


Figure 5. Typical Current Output Curve
(After Barns (1979))

been referred to as the limiting current (Hitchman, 1979) or as the diffusion limiting region (Barnes, 1979). As described by both authors, when operating a cell at the potentials corresponding to this plateau region, all the reactions are able to proceed such that no reactants will remain in suspension near the cathode's surface.

This region has been described by others as the region where all reactant material is electrolyzed (Morgan and Bewtra, 1962). Through this type of operation, complete oxidation takes place and the corresponding current output is solely dependent on the flux of oxygen entering the probe or passing through the membrane.

In 1957, the Clark probe was further refined by Carritt and Kanwasher, who developed a temperature compensation method (Mancy and Westgarth, 1961). It was found that the polarographic membrane probe could increase its output current by as much as 1% to 6% with each 1°C change in temperature. Changing membrane permeability is the primary cause of this change in current output. The phenomenon can be clearly seen in Figure 6 (Hitchman, 1979).

The polarographic membrane probe actually measures the fugacity of the oxygen in the solution (Hitchman, 1979). These values are then assumed to be equal to the partial pressure of the oxygen. There are conditions, however, when fugacity and partial pressure are not equivalent. The ratio of fugacity to

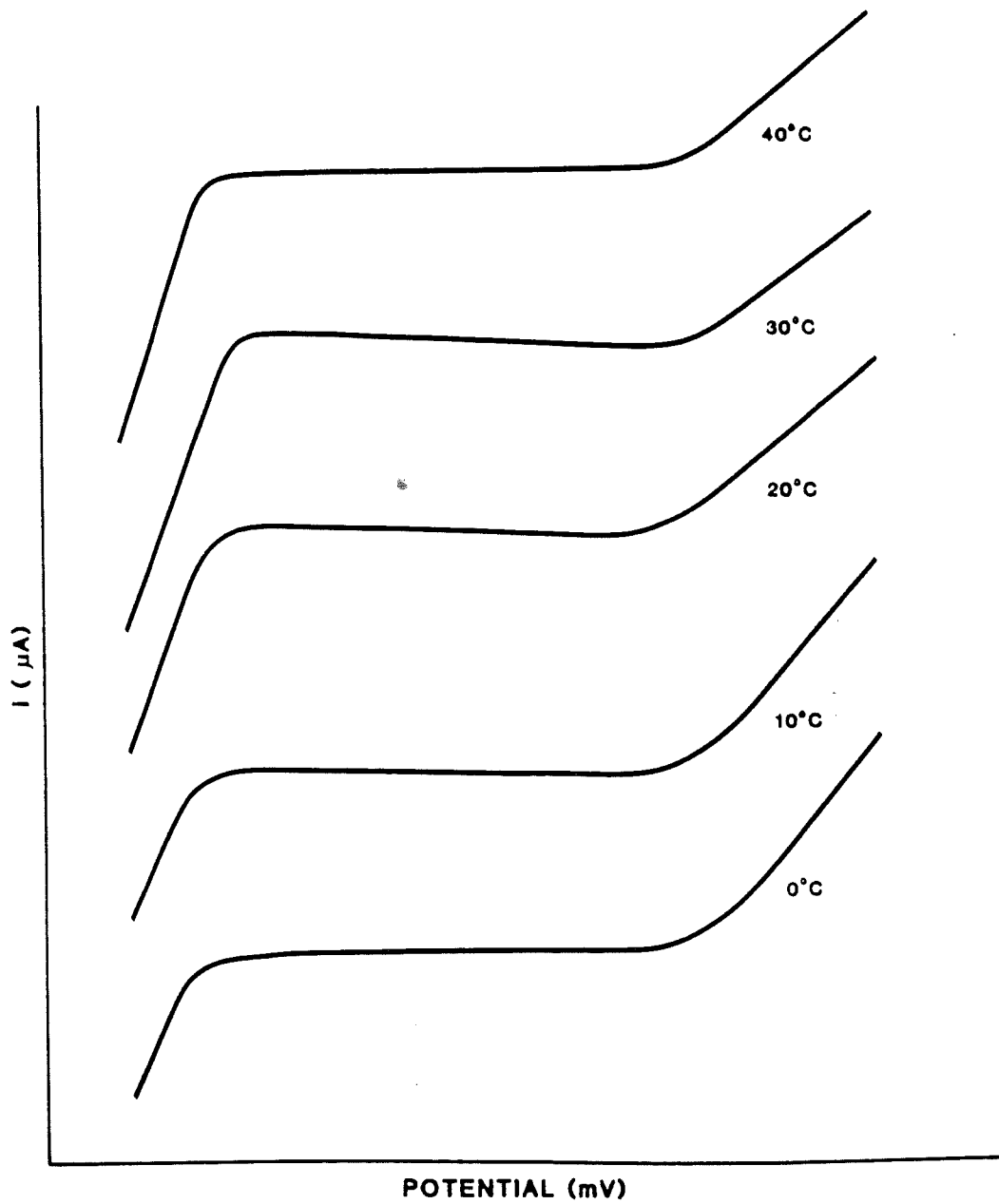


Figure 6. Temperature Effect on Current Output
(After Hitchman (1979))

partial pressure has been termed the activity coefficient (Snoeyink and Jenkins, 1980). This coefficient varies with the ionic concentration in the solution. Consequently, for water containing a high concentration of ionic material, such as salt water, the probe's output must be adjusted to account for this change in the activity coefficient. Many probe manufacturers provide for both temperature and salinity correction on their instruments.

A cell, as has been described, is typically operated at a voltage well within the corresponding limiting current region for the cell (Rand and Heukelekian, 1951). In this area, the rate of transport of oxygen toward the cathode obeys Fick's law. Also in this region, minor fluctuations in operation voltage will not significantly effect the current output of the instrument.

The diffusion field of the probe, under steady-state conditions is illustrated in Figure 7. The involved kinetics are composed of the transport properties of the polymer membrane, the transport properties of the electrolyte and the geometry of the electrolyte and the membrane layers (Aiba, 1973). This can be seen from Figure 7, which shows the oxygen partial pressure at each point within the system.

In Figure 7, K_E , K_M , and K_L , represent the oxygen transport coefficients of the electrolyte, the membrane and the liquid, respectively. K'_o and K_b represent the transport coefficients on the inside and outside of the membrane,

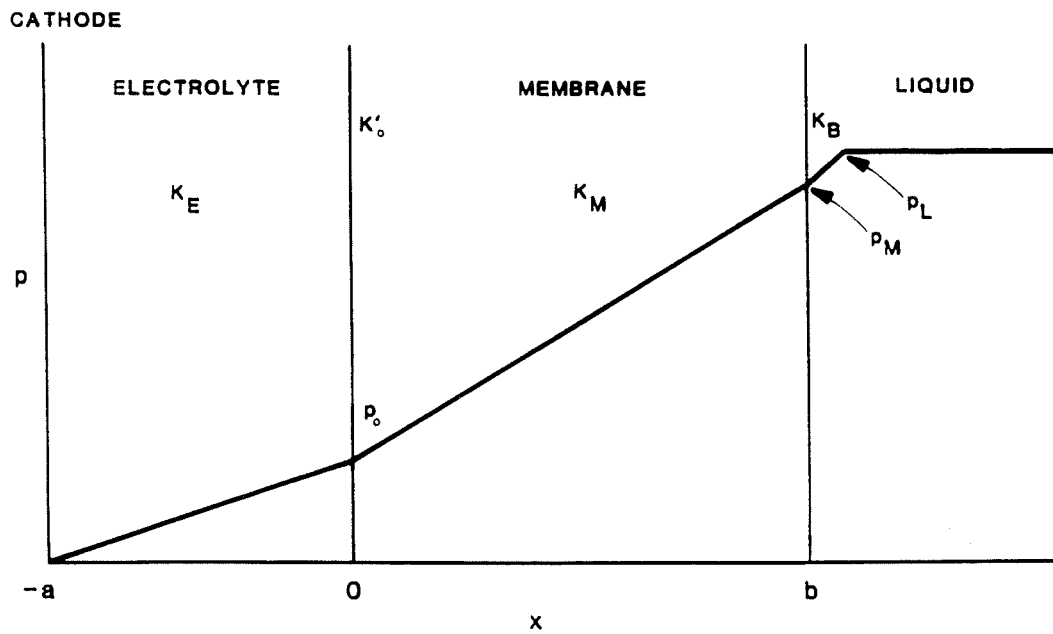


Figure 7. Probe Diffusion Field
(After Aiba (1973))

respectively. P_o , P_m , and P_l are the oxygen partial pressures on the inside surface of the membrane, the outside surface and the liquid medium, respectively.

With this model in mind, an expression for oxygen flux through each part of the system can be derived using Fick's law:

$$N = K_L (P_L - P_b) \quad \text{the flux through the liquid} \quad (8)$$

$$N = K_m (P_L - P_b) \quad \text{the flux through the membrane} \quad (9)$$

$$(P_m/b) (P_b - P_o) \quad P = \text{membrane permeability,}$$

$b = \text{thickness of membrane}$

$$N = K_E (P_L - 0) \quad \text{the flux through the electrolyte} \quad (10)$$

If we assume that K_L and K_b' are much greater than the others, meaning that these points create relatively little resistance to oxygen mass transfer (Aiba, 1969), the following equation is obtained:

$$N = K_o (P_L - P_o) \quad (11)$$

where

$$1/K_o = 1/K_L + 1/K_n \quad (12)$$

As shown in Equation (12), the overall oxygen mass transfer coefficient within the cell is dependent on the mass transfer coefficient of the liquid medium or water sample. This could cause the resulting current output from the probe to be sensitive to conditions of the water, such as viscosity. Aiba (1969) calculated that this over-sensitivity would not occur for values of

$$K_o/K_l \leq 0.05 \tag{13}$$

As can be seen by Equation (9) the oxygen flux of the membrane could be increased by either increasing the permeability of the membrane or decreasing its thickness. It has been reported in the literature (Barnes, 1979) that a 25 μm polyethylene membrane caused a response time of six seconds, while a 25 μm polyethylene terephthalate membrane caused a response time of 300 seconds on the same probe. There are several reasons, however, why this higher flux can not be practically attained. The higher flux would lead to the rapid oxygen depletion from the membranes interface with the test solution. It would also cause the anode to age considerably faster and possibly cause a shift in the reaction potential of the system (Barnes, 1979).

Another important factor to consider when working with membrane covered probes is stirring. The test solution must be kept agitated at all times to provide a constant flux of oxygen through the membrane. Requirements for agitation are noted in the Standards for the Clean Water Test (ASCE, 1984).

C. Nonsteady-State Probe Response

There are two cases referred to in the literature for the nonsteady-state applications of the polarographic probe (Hitchman, 1978). These cases are: (1) when the instrument is first turned on, or when a potential is first applied across the anodes, and (2) when the dissolved oxygen concentration is changing in the test solution. The effect of both of these conditions on the probe's diffusion layers is shown in Figure 8.

Typically, as discussed earlier, the diffusivity of the membrane is considered the time limiting factor. The relationship between this diffusivity and time lag as has been shown in the literature (Hitchman, 1978) as:

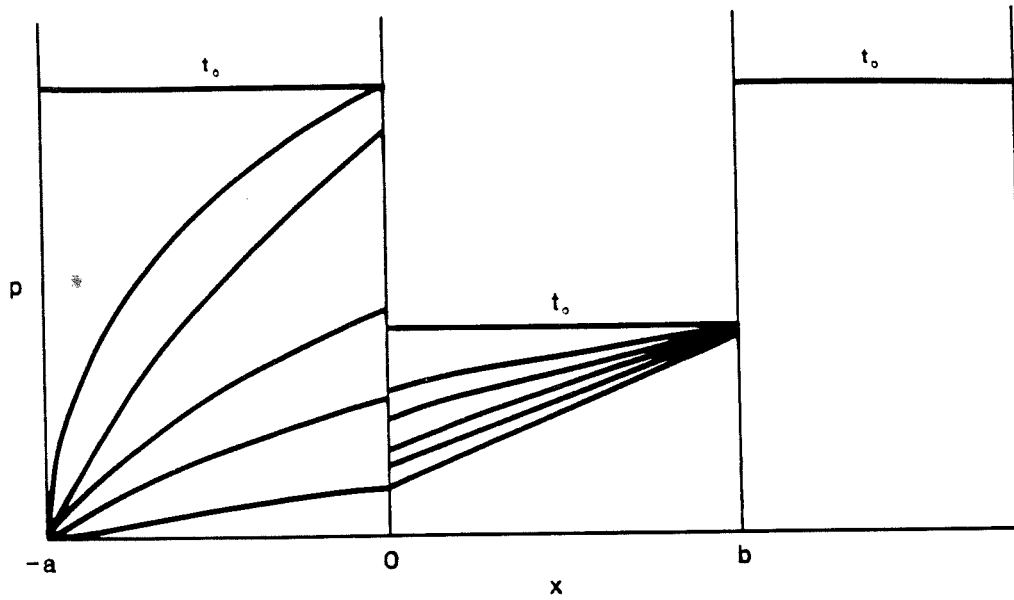
$$t = b^2/D_m \quad (14)$$

b = thickness of the membrane

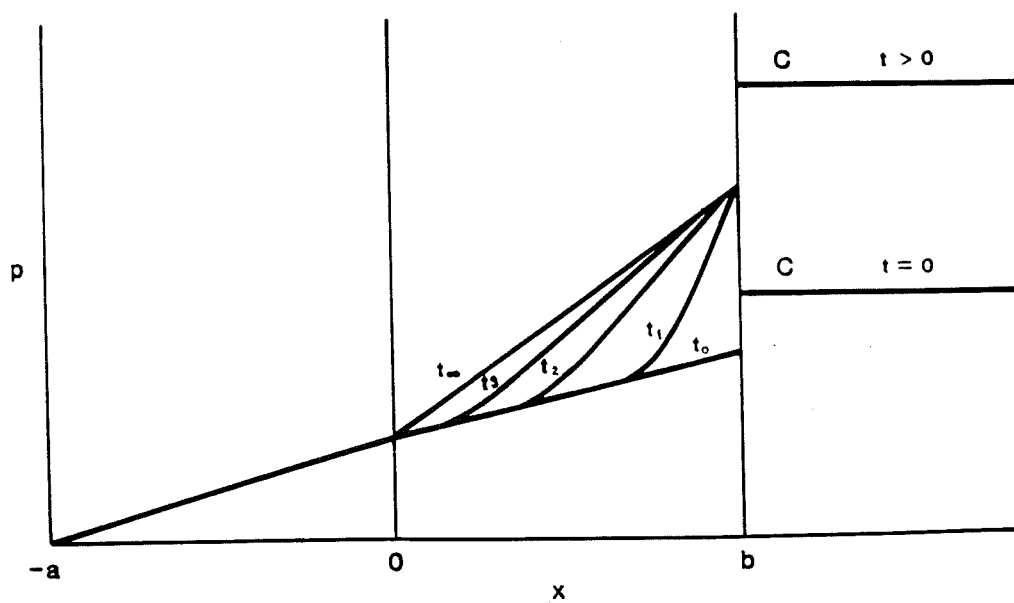
D_m = diffusivity of oxygen

This relationship has been shown graphically by others (Aiba and Huang, 1969) and can be seen in Figure 9. The equation for this relationship is as follows:

$$i_t = nFAP_m \left(\frac{P_s}{b} \right) - \left\{ 1 + 2 \sum_{n'=1}^{\infty} (-1)^{n'} e^{-n'^2 \pi^2 \frac{D_m t}{b^2}} \right\} \quad (15)$$



CONDITION 1



CONDITION 2

Figure 8. Probe Diffusion Layers
(After Hitchman (1978))

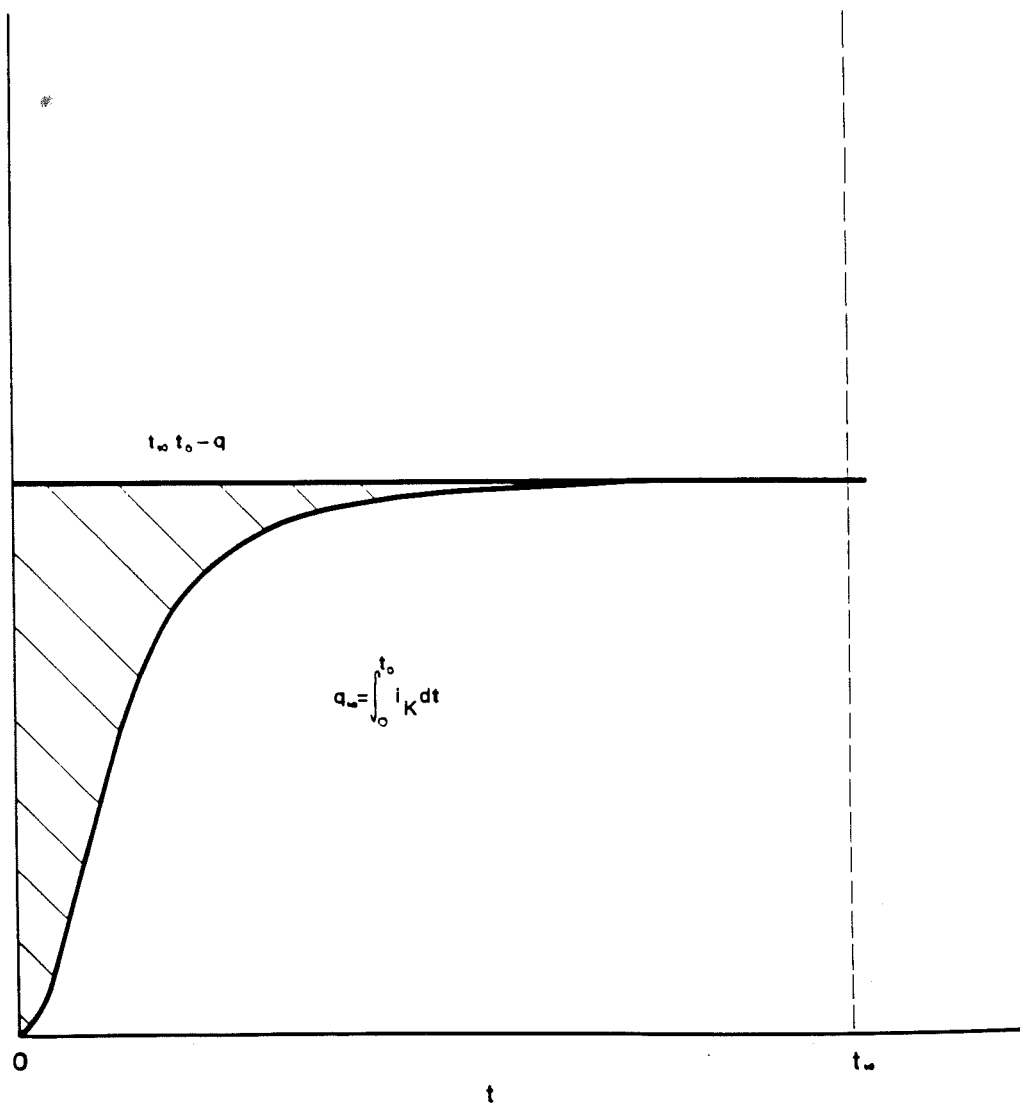


Figure 9. Nonsteady-State Probe Response
(After Aiba and Huang (1969))

i_t = current

P_m = permeability of membrane

P_s = partial pressure of O_2 in sample

n' = positive integer

$$D_m = \frac{b^2 i_\infty}{6(i_{in} - t_o q_\infty)} \quad (16)$$

$$q_\infty = \int_0^{t_o} i_t dt \quad (17)$$

i_{IN} = initial current

t_o = initial time

While this research is mainly concerned with the effects of probe lag on oxygen transfer testing, it is interesting to note that Barnes (1979) developed a method to evaluate and quantify this lag mathematically, relating the values of oxygen flux across the membrane as a function of time. Barnes's method utilizes nonlinear least squares fit analysis to first determine the total lag time, then to find the lag due to the electrolyte and that due to the membrane.

D. Summary

The nonsteady-state clean water test is a popular way of evaluating the oxygen transfer rates and efficiencies of aeration systems. The polarographic oxygen electrode is a practical method for the required measurements of dissolved oxygen concentrations throughout the test. The literature has shown that the lag time associated with this polarographic measurement can influence the estimated transfer rate.

The working principal and evolution of polarographic oxygen probe has been discussed. We have examined the kinetics involved with the operation of the polarographic probe and have found the fundamental basis for the lag time associated with the probe.

III. RESEARCH PROCEDURE

To quantify and analyze the effects of probe lag, data were obtained in UCLA's Water Quality Laboratory. The experimental data were augmented by computer simulations.

A. Experimental Procedures

Two types of physical tests were performed. The first test, termed the lag test, was used to determine the time constant for the oxygen probes using various membranes and membrane combinations. The second test performed was the standard ASCE (1984) clean water test. This test was used for the determination of the oxygen transfer coefficient $K_L a$ values of the system.

1. Apparatus

The basic apparatus used for the tests is shown in Figure 10. It consisted of a cylindrical nine gallon Pyrex glass tank which had an inside diameter of 15.5 inches and a depth of 11.75 inches. This tank was mounted upon four Magnestir Model S8290 mixers manufactured by Scientific Products.

A diffused air aeration system was installed within the tank. This system consisted of three one inch diameter spherical stones (Fischer Scientific, catalog number 11-139A). These stones were connected together and supported by 1/4

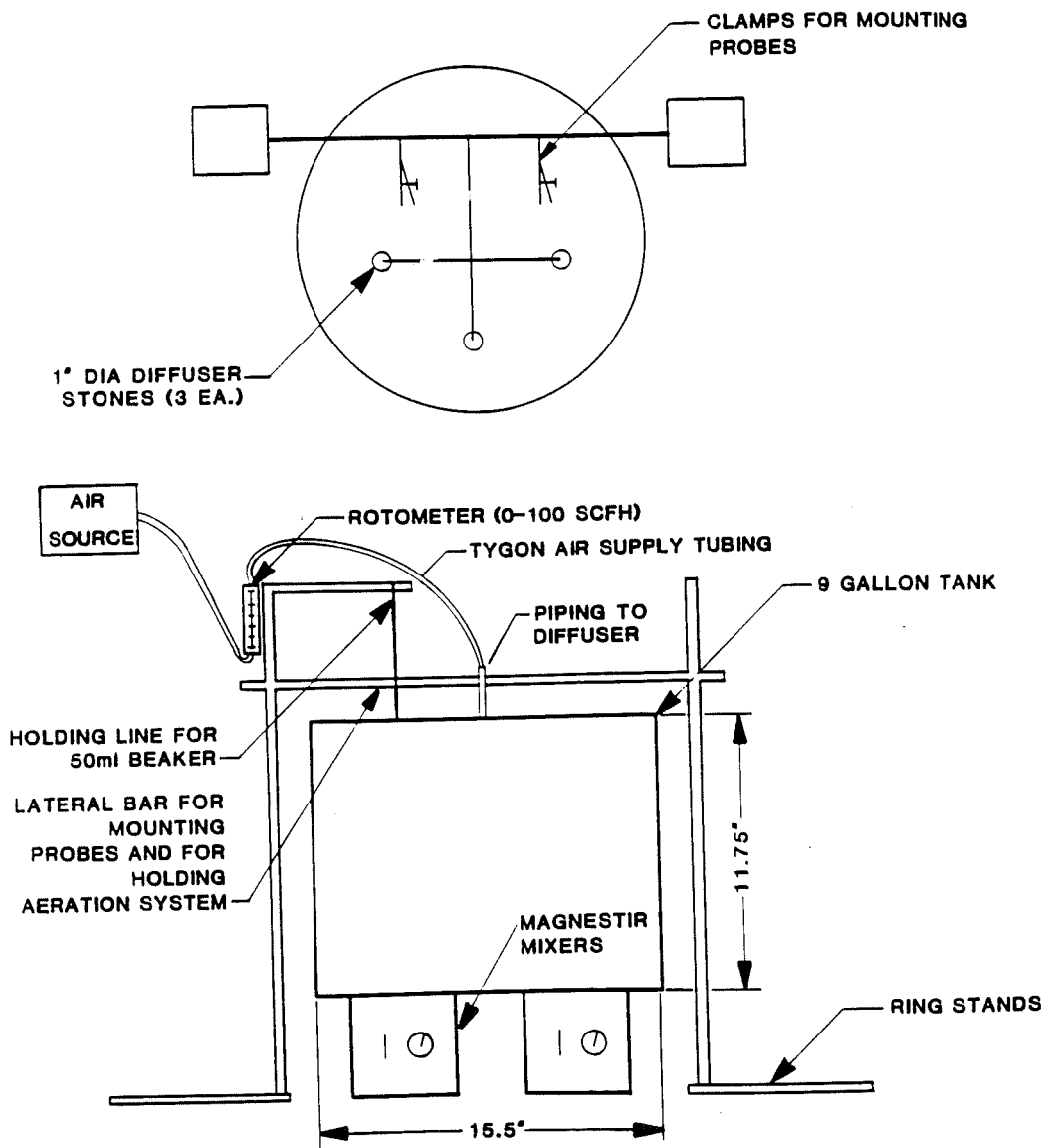


Figure 10. Basic Test Apparatus

inch stainless steel tubing and fittings as detailed in Figure 11.

The air for this system was supplied by the laboratory's compressed air system. Tygon tubing was used to connect the diffusers and rotameter, as shown in Figure 11. A Dwyer Rotameter (catalog number VFA 8B) was used to control air flow rate.

Dissolved oxygen concentration was measured with two YSI Model 5739 dissolved oxygen probes. The probes were connected to YSI Model 51B oxygen meter analyzers. Both analyzers were electrically modified to use an external recorder.

This output signal from the analyzer was recorded and displayed using an IBM personal computer, modified with Lab Tech Notebook hardware and software (Laboratory Technologies Corporation, Wilmington, MA.). The dissolved oxygen signal was amplified and conditioned using a Micro Byte operational amplifier (Model 852P), revision number 852P, serial number 9514.

2. Test Initialization Procedure

The lag tests and the clean water tests were performed sequentially. Typically a group of lag tests were performed followed by a group of clean water tests. Prior to this series of tests however, the equipment was prepared and calibrated. This initial preparation is referred to as the test initialization

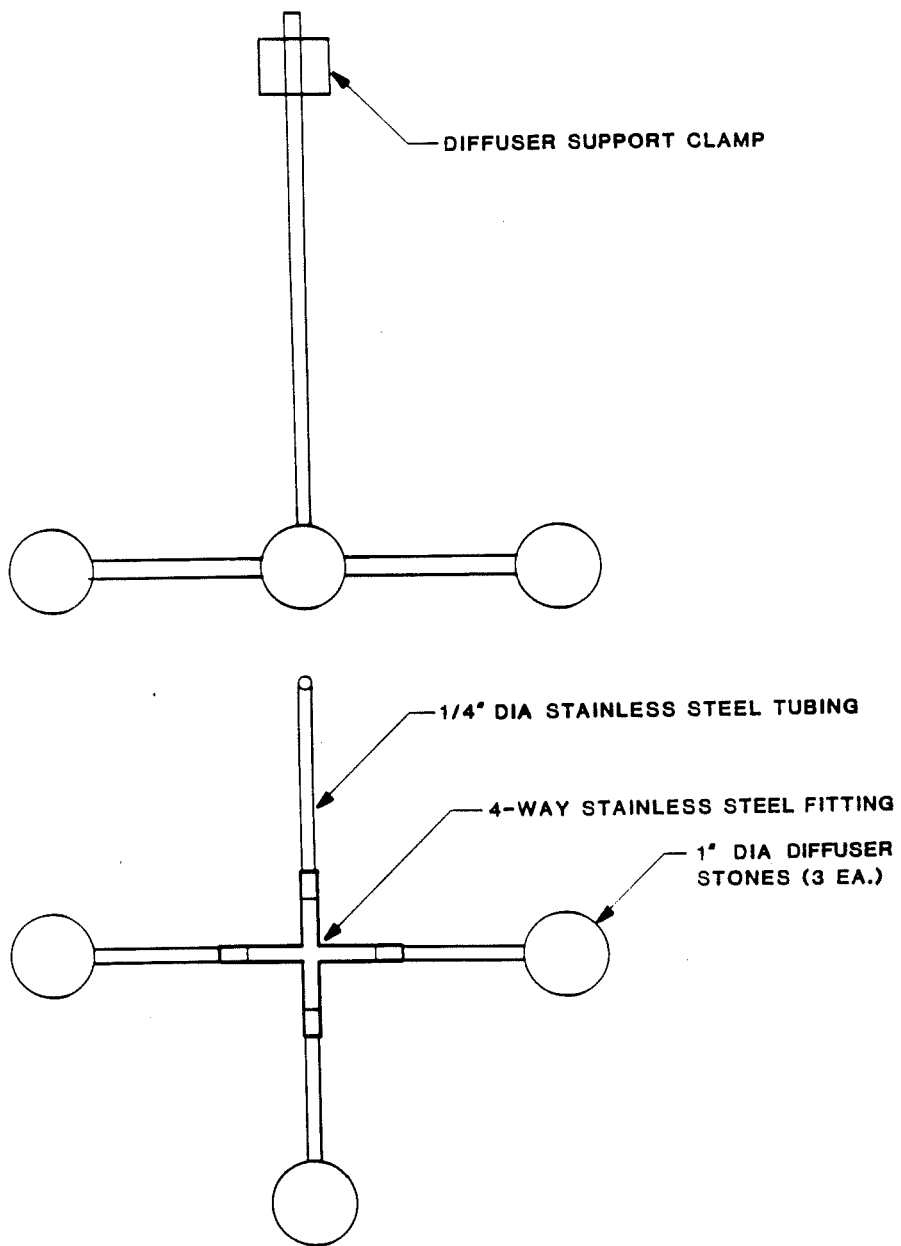


Figure 11. Test Apparatus Diffused Air System

procedure.

The desired membranes or membrane combinations were attached to the probes. As per the manufacturer's instructions, the electrolyte was completely flushed out and refilled prior to the connection of the membrane. Before concluding this step it was observed that there were no air bubbles beneath the membrane surface and that the membrane was pulled tight such that no wrinkles existed.

The DO meters were then adjusted to their zero scale point using their zero adjust. After insuring that the probes were adequately adjusted to this zero value, the computer recording equipment was checked and calibrated. Three, 20 second tests were conducted simultaneously using this zero signal input. A dissolved oxygen signal was sampled each second during the 20 second period. The reading for each of the tests, for each probe channel, was then averaged and used for the determination of the software's offset factor. After setting this factor, a zero test was run again to verify that this offset factor did in fact zero the recorded signals.

Next the full scale was adjusted on the DO meters. After it was correctly adjusted, the recorder equipment was correspondingly checked and adjusted. Again three, 20 second tests were performed with dissolved oxygen values being sampled each second. The values for each of the three tests was also

averaged for each of the probe's channels. This value was accordingly used for the determination of the software's scale factor adjustment. Following this adjustment a 20 second test was run again to insure that the DO meters full scale output was correctly displayed.

After the adjustment of the recorder software, the probes themselves were calibrated. This calibration was performed by immersing them in a BOD bottle containing water which had been aerated for a minimum of two hours. This water was continuously mixed using a magnet stir. The probes were then adjusted to the corresponding saturation dissolved oxygen value for this water's measured temperature. The analyzer's temperature correction was also adjusted to this measured temperature.

After each probe was calibrated, the 20 second recorder test was again run to insure that all of the previous adjustments had been correct, and that the recorder's reading was the actual dissolved oxygen being read by the probe. Records were kept of all of the these initialization tests to insure that the equipment was not experiencing any major changes.

3. The Probe Lag Test

After the test initialization procedure was completed, a series of probe lag tests was typically performed. The object of these tests was to create an

instantaneous change to the dissolved oxygen concentration being measured by the probe. The probes response was accordingly recorded.

Both probes were mounted in the test tank such that their membranes faced downwards, and their tips were submerged approximately one inch below the water's surface. Beneath the probe being tested, a 50 ml Pyrex beaker was hung submerged as shown in Figure 12. This beaker was held such that its rim was just touching the tank's water surface, not allowing the water inside and outside to mix. The water within the beaker was then removed using a 100 ml pipet. This water was replaced with water having a significantly different dissolved oxygen concentration from that in the tank.

Tests were conducted with the beaker water DO concentration both higher and lower than that of the tank. To poise the probe's initial condition at greater DO concentration than its final condition, the DO in the test tank was deoxygenated by bubbling nitrogen gas through the aeration system. When testing with the opposite conditions, water deoxygenated with nitrogen was kept in a 400 ml beaker and placed in the 50 ml beaker prior to each test.

To create the desired instantaneous change in the dissolved oxygen being measured by the probe, the beaker was rapidly lowered into the tank. The water within the beaker would quickly be dispersed throughout the tank, and the probe was immediately subjected to the tank dissolved oxygen concentration.

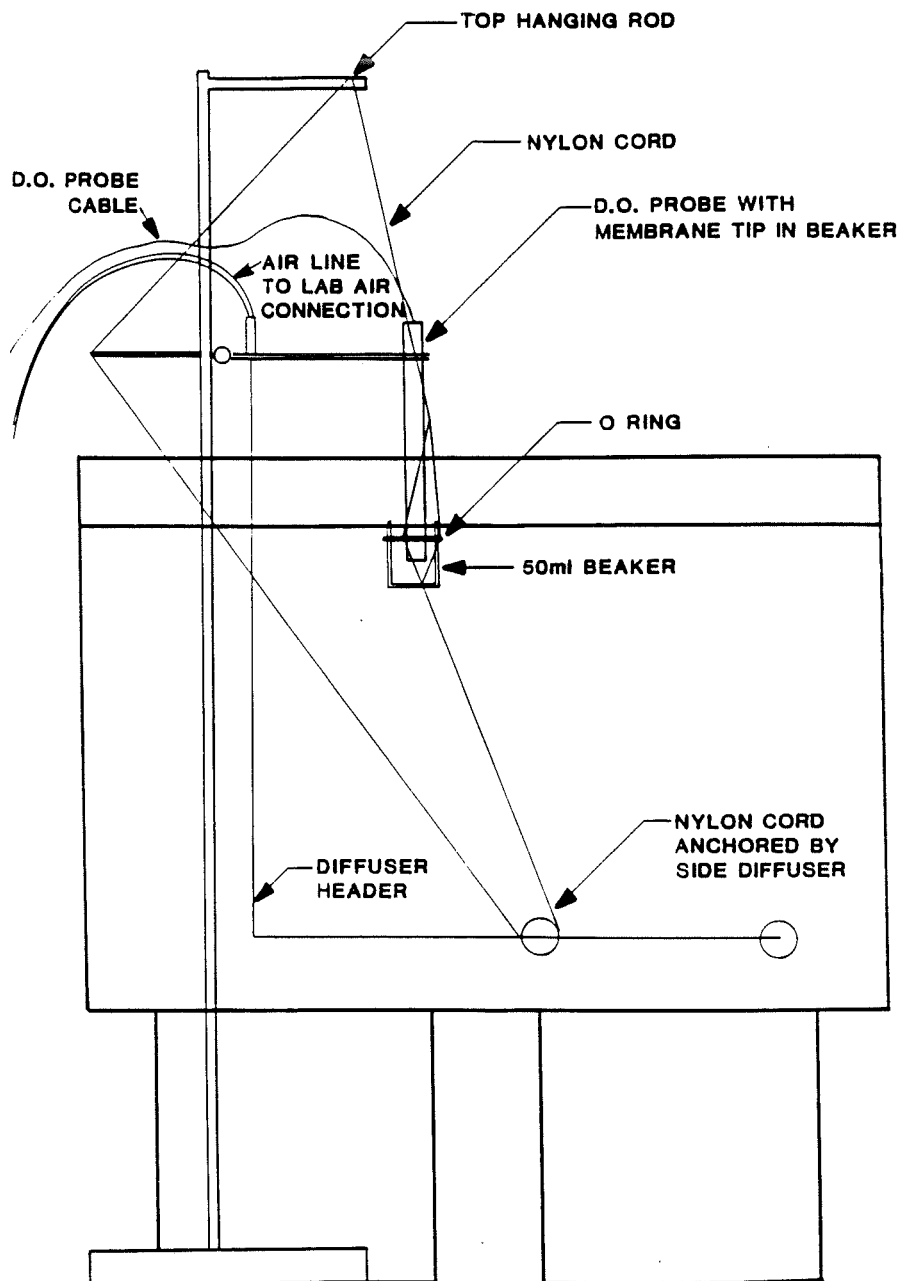


Figure 12. Lag Test Procedure

These tests were run for periods of 200 seconds with dissolved oxygen concentration being recorded at one second increments. Typically the beaker was lowered approximately 20 seconds after the initiation of recording. Stirring bars at the bottom of the tank were utilized to recirculate the water moving past the probe's membrane. The temperature was also periodically monitored and the analyzers were periodically adjusted to correct for any changes.

Each lag test was performed on each probe a minimum of three times. They were performed using ordinary tap water which was periodically monitored for both temperature changes and changes in clarity.

The recorded data from this test, which consisted of the concentration versus time data was used to calculate the probes time constant. As discussed in the literature reviewed, the probe lag was considered first order, and calculated as such. This first order time lag can be represented by Equation (18).

$$\ln \frac{C_f - C}{C_f - C_i} = -t/\tau \quad (18)$$

where

- C_f = final concentration reading of the probe
- C_i = initial reading
- C = concentration value at each time increment
- t = time

These tests were run for periods of 200 seconds with dissolved oxygen concentration being recorded at one second increments. Typically the beaker was lowered approximately 20 seconds after the initiation of recording. Stirring bars at the bottom of the tank were utilized to recirculate the water moving past the probe's membrane. The temperature was also periodically monitored and the analyzers were periodically adjusted to correct for any changes.

Each lag test was performed on each probe a minimum of three times. They were performed using ordinary tap water which was periodically monitored for both temperature changes and changes in clarity.

The recorded data from this test, which consisted of the concentration versus time data was used to calculate the probes time constant. As discussed in the literature reviewed, the probe lag was considered first order, and calculated as such. This first order time lag can be represented by Equation (18).

$$\ln \frac{C_f - C}{C_f - C_i} = -t/\tau \quad (18)$$

where

- C_f = final concentration reading of the probe
- C_i = initial reading
- C = concentration value at each time increment
- t = time

τ = time constant.

To solve for τ the left side of this equation was plotted against time as shown typically by Figure 13. The slope of this line was then calculated and the time constant was considered to be the inverse of this slope.

As can be seen by Figure 13, the slope was not entirely a straight line. This was assumed to be due to other lag forces which occurred as the dissolved oxygen gradient decreased. It was determined, however, that the controlling lag on the probe was first-order. This determination was based on probes unquestionable first-order response when extremely high values were involved, as when multiple membranes are attached in series. This response is illustrated by Figure 14.

To check for a possible second-order lag, this same value was plotted against the natural logarithm of the time. A sample of these plots is shown in Figure 15. As can be seen, this attempt was without success.

4. The Clean Water Test

Several clean water tests were performed during each of the testing periods. Here, both probes were suspended and submerged by their cables. The probes were oriented so that their membranes faced upward, and were approximately five inches below the water's surface. The probes were hung in

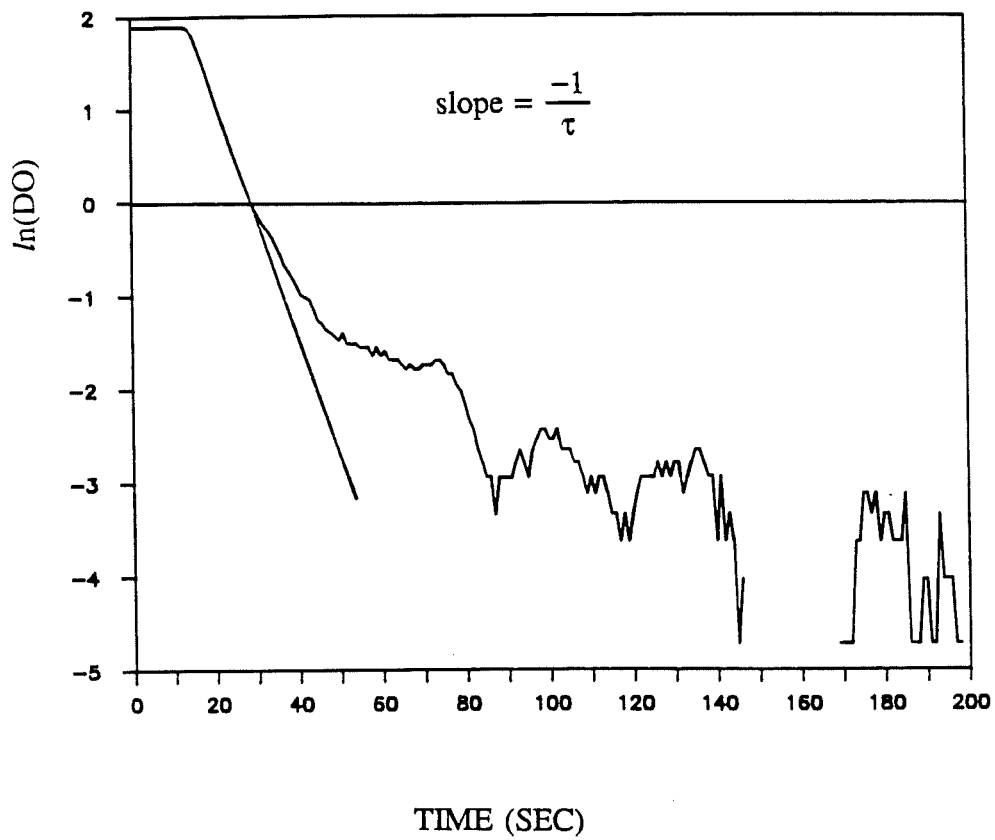


Figure 13. Time Constant Calculation

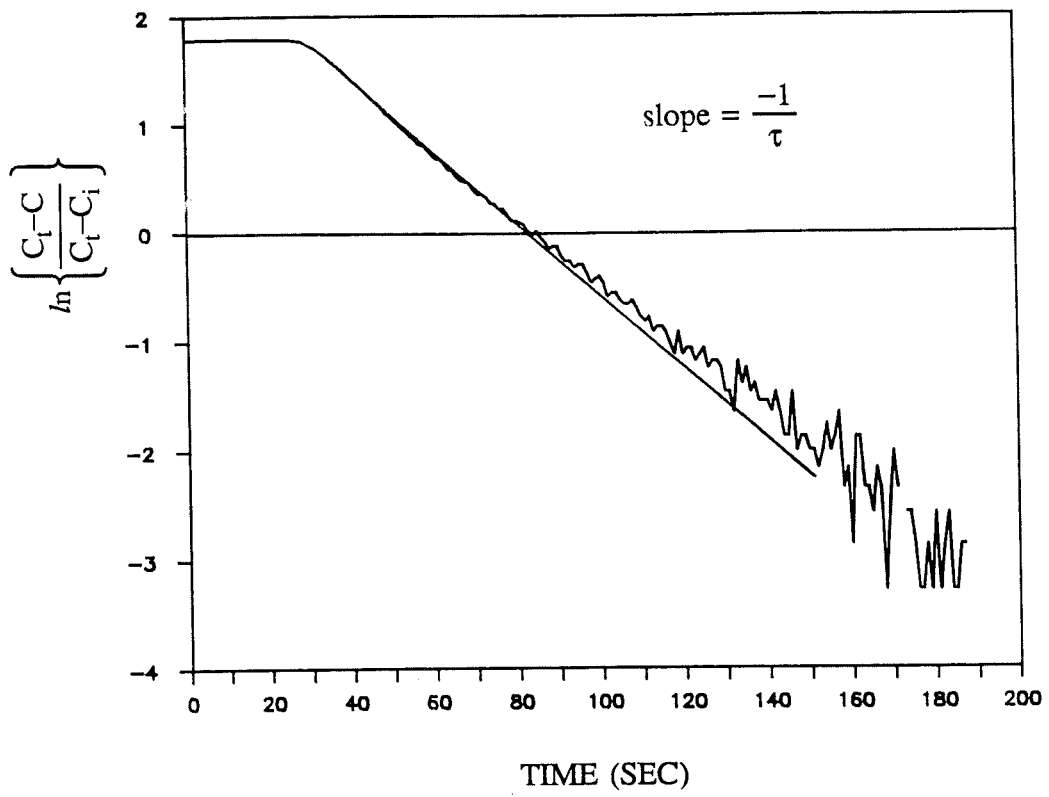


Figure 14. Time Constant Calculation

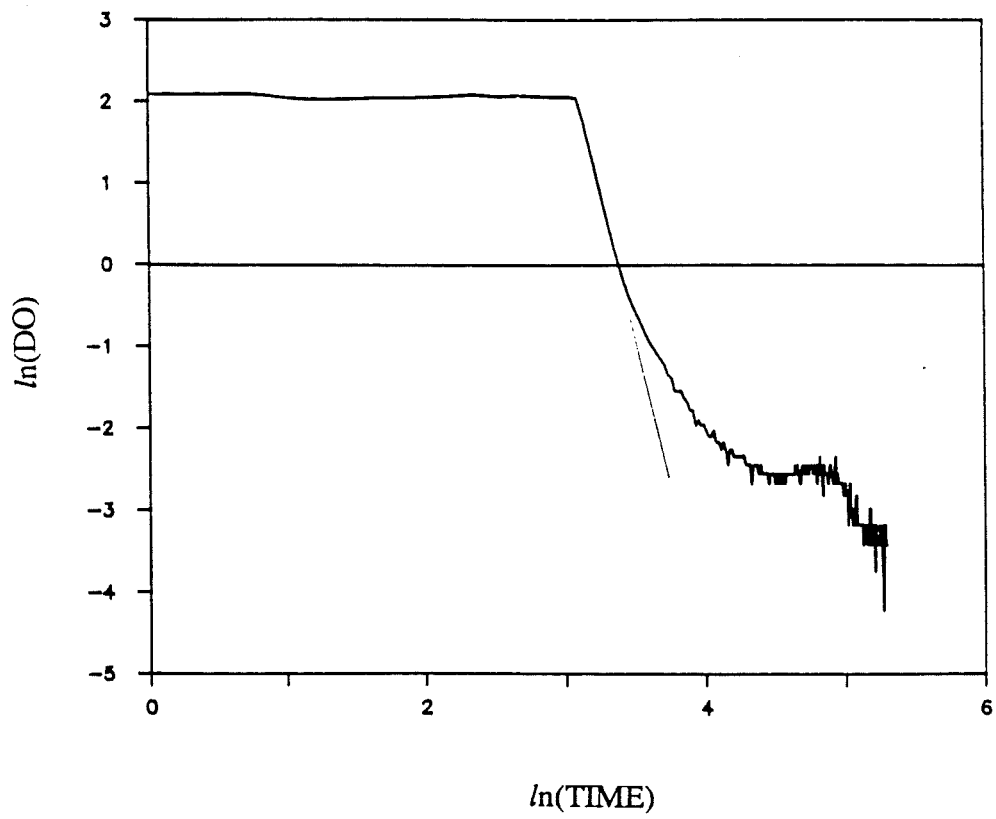


Figure 15. Typical Log-Log Response for 2nd Order Time Constant

this inverted manner to prevent air bubble formation on the membrane. The probes were placed such that they were at least four inches from the edge of the tank and away from direct exposure to the rising diffuser bubbles.

Between tests, water in the tank was deaerated using nitrogen gas. Again nitrogen was piped through the tank's diffuser system until the dissolved oxygen content was reduced to below 1.0 mg/L. The water temperature was continuously monitored and the analyzers were continuously adjusted for temperature correction.

After this initial set-up procedure, the recording equipment was started and the air flow was turned on and set at an intended flow rate. During the tests, the magnetic stirring rods were operated to insure adequate circulation and to allow for the proper mixing around the probe.

These tests were allowed to continue for ten minutes with their dissolved oxygen values being recorded each second. This procedure was then repeated for the remaining tests. As with the probe lag tests, tap water was used. This water quality was continuously monitored and replaced as necessary. Typical results obtained with this test for two probes with different membranes are shown in Figure 16.

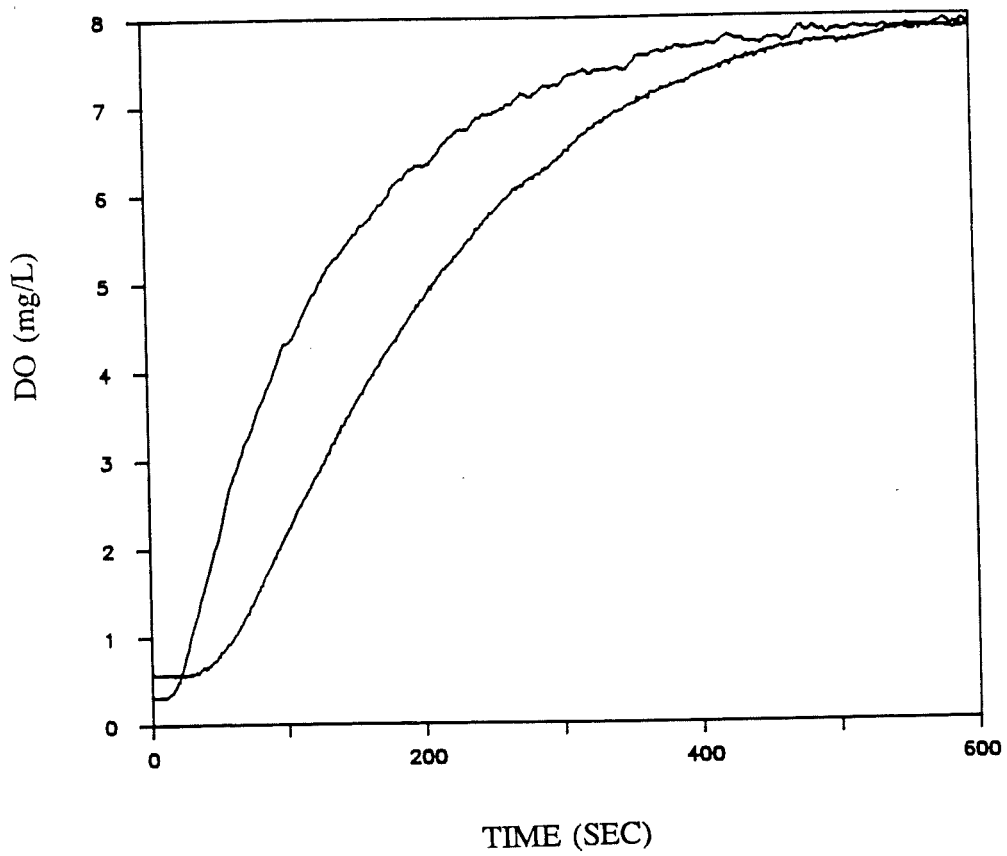


Figure 16. Clean Water Test Results for Two Different Types of Membranes

The $K_L a$ values were later determined for each probe during each test conducted. This was done utilizing the exponential method as described by the ASCE Standard. Here a nonlinear least squares fit program was employed to perform the calculations.

B. Probe Simulation

In order to simulate probe responses beyond the capability of the experiment equipment, and to confirm the experimental results with theory, probe lag was simulated using CSMP III, (IBM 1972). The following set of differential equations were solved using CSMP III.

$$\frac{dC}{dt} = K_L a (C_{\infty}^* - C) \quad (19)$$

$$\frac{dC_{p_1}}{dt} = \frac{(C - C_{p_1})}{\tau} \quad (20)$$

$$\frac{dC_{p_2}}{dt} = \frac{(C - C_{p_2})}{\tau} \quad (21)$$

where

- C = actual dissolved oxygen concentration,
- C_{p_1} = dissolved oxygen concentration indicated by Probe 1
- C_{p_2} = dissolved oxygen concentration indicated by Probe 2
- τ_1 = time constant for Probe 1

τ_2 = time constant for Probe 2.

The equations were integrated using the fourth order variable step Runge-Kutta procedure. Values of C , C_p , and C_{p_2} were printed and appropriate intervals and analyzed using the ASCE exponential method. Ranges of $K_L a$, τ_1 and τ_2 were selected in the range of the experimental results in order to verify them. Additionally, values outside of this range were also used in order to extend the theories developed later.

IV. EXPERIMENTAL RESULTS

The results which were obtained in the previously discussed manner are shown in Tables 1 and 2. Table 1 shows the experimentally determined probe responses and $K_L a$'s. Table 2 shows the $K_L a$'s obtained from simulated probe responses. The values of τ listed for the experimental results are the average of the several values obtained during the preceding probe lag tests. The $K_L a$ values from both tables were first estimated using all data points (no truncation) and later estimated after truncating the data at 20% of the equilibrium DO concentration. The results of each are shown. The ASCE (1984) standard permits "low side" truncation up to 20% of C_∞^* .

The ratio of $K_L a$'s obtained from a test probe (a slow probe) and a standard probe (fast probe) are also shown in Tables 1 and 2. This ratio is shown for $K_L a$'s estimated with truncated and untruncated data. For the purpose of comparison, all results are compared to a standard probe, which has a true constant of about 7.7 seconds.

Figure 17 compares the $K_L a$ rating estimated from the simulated data. This plot shows how the ratio varies with different time constants and at different values of $K_L a$. Figure 18 plots this $K_L a$ ratio for both the experimental and simulated results against the $\tau K_L a$ values. This plot is performed for both

Table 1. Summary of Experimental Results

Test	Membrane Type	τ (sec)	$K_L a^+$ (*10 ³) (sec ⁻¹)	$K_L a^{++}$ (*10 ³) (sec ⁻¹)	Ratios		Product ($\tau K_L a_T$)
					$\frac{K_L a^+}{K_L a_T}$	$\frac{K_L a^{++}}{K_L a_T}$	
LAG525A	B	34.2					
LAG525B	B	27.9					
LAG525C	B	31.1					
LAG525D	A	7.8					
LAG525E	A	7.6					
LAG525F	A	7.7					
CLN525A	A	31.0	6.79	5.32	0.77	0.68	0.275
	B	7.7	8.86	7.88			
CLN525B	A	31.0	7.15	5.94	0.75	0.67	0.295
	B	7.7	9.50	8.93			
CLN525C	A	31.0	6.87	5.69	0.77	0.68	0.275
	B	7.7	8.88	8.36			
CLN525D	A	31.0	7.34	6.17	0.76	0.68	0.300
	B	7.7	9.68	9.12			
CLN525E	A	31.0	7.30	6.12	0.78	0.68	0.291
	B	7.7	9.38	8.95			
CLN525F	A	31.0	7.22	5.98	0.77	0.68	0.291
	B	7.7	9.37	8.80			
LAG524A	F	20.6					
LAG524B	F	19.2					
LAG524C	F	16.7					
LAG524D	A	8.1					
LAG524E	A	7.5					
LAG524F	A	8.2					
LAG524G	F	18.3					
CLN524A	F	18.7	7.76	6.81	0.85	0.79	0.172
	A	7.9	9.17	8.61			
CLN524B	F	18.7	8.42	7.24	0.87	0.80	0.182
	A	7.9	9.70	9.02			
CLN524C	F	18.7	8.47	7.31	0.89	0.82	0.178
	A	7.9	9.50	8.91			

Table 1. Summary of Experimental Results (continued)

Test	Membrane Type	τ (sec)	$K_L a^+$ (*10 ³) (sec ⁻¹)	$K_L a^{++}$ (*10 ³) (sec ⁻¹)	Ratios		Product ($\tau K_L a_T$)																																																																																																																																																																																												
					$\frac{K_L a^+}{K_L a_T}$	$\frac{K_L a^{++}}{K_L a_T}$																																																																																																																																																																																													
CLN524D	F	18.7	7.87	6.26	0.84	0.79	0.175																																																																																																																																																																																												
	A	7.9	9.37	7.96				CLN524E	F	18.7	8.12	7.25	0.83	0.77	0.183	A	7.9	9.81	9.36	CLN524F	F	18.7	8.09	7.19	0.85	0.80	0.178	A	7.9	9.53	9.04	CLN524G	F	18.7	7.84	6.89	0.84	0.80	0.174	A	7.9	9.28	8.64	CLN524H	F	18.7	8.43	7.44	0.91	0.81	0.173	A	7.9	9.25	9.24	CLN524I	F	18.7	8.35	7.43	0.87	0.81	0.179	A	7.9	9.58	9.13	LAG523A	E	52.2						LAG523B	E	52.3						LAG523C	E	51.6						LAG523D	A	8.5						LAG523E	A	8.8						LAG523F	A	7.9						CLN523A	E	52.1	5.95	4.07	0.69	0.50	0.446	A	8.4	8.58	8.16	CLN523B	E	52.1	6.76	4.78	0.72	0.53	0.490	A	8.4	9.42	8.98	CLN523C	E	52.1	6.20	4.68	0.65	0.52	0.494	A	8.4	9.48	9.03	CLN523D	E	52.1	6.19	4.24	0.69	0.50	0.468	A	8.4	8.99	8.45	CLN523E	E	52.1	6.47	4.62	0.67	0.50	0.504	A	8.4	9.68	9.23	CLN523F	E	52.1	6.23	4.59	0.66	0.51	0.488	A	8.4	9.38	9.03	CLN523G	E	52.1	6.15	4.41	0.67	0.51	0.476
CLN524E	F	18.7	8.12	7.25	0.83	0.77	0.183																																																																																																																																																																																												
	A	7.9	9.81	9.36				CLN524F	F	18.7	8.09	7.19	0.85	0.80	0.178	A	7.9	9.53	9.04	CLN524G	F	18.7	7.84	6.89	0.84	0.80	0.174	A	7.9	9.28	8.64	CLN524H	F	18.7	8.43	7.44	0.91	0.81	0.173	A	7.9	9.25	9.24	CLN524I	F	18.7	8.35	7.43	0.87	0.81	0.179	A	7.9	9.58	9.13	LAG523A	E	52.2						LAG523B	E	52.3						LAG523C	E	51.6						LAG523D	A	8.5						LAG523E	A	8.8						LAG523F	A	7.9						CLN523A	E	52.1	5.95	4.07	0.69	0.50	0.446	A	8.4	8.58	8.16	CLN523B	E	52.1	6.76	4.78	0.72	0.53	0.490	A	8.4	9.42	8.98	CLN523C	E	52.1	6.20	4.68	0.65	0.52	0.494	A	8.4	9.48	9.03	CLN523D	E	52.1	6.19	4.24	0.69	0.50	0.468	A	8.4	8.99	8.45	CLN523E	E	52.1	6.47	4.62	0.67	0.50	0.504	A	8.4	9.68	9.23	CLN523F	E	52.1	6.23	4.59	0.66	0.51	0.488	A	8.4	9.38	9.03	CLN523G	E	52.1	6.15	4.41	0.67	0.51	0.476	A	8.4	9.14	8.65								
CLN524F	F	18.7	8.09	7.19	0.85	0.80	0.178																																																																																																																																																																																												
	A	7.9	9.53	9.04				CLN524G	F	18.7	7.84	6.89	0.84	0.80	0.174	A	7.9	9.28	8.64	CLN524H	F	18.7	8.43	7.44	0.91	0.81	0.173	A	7.9	9.25	9.24	CLN524I	F	18.7	8.35	7.43	0.87	0.81	0.179	A	7.9	9.58	9.13	LAG523A	E	52.2						LAG523B	E	52.3						LAG523C	E	51.6						LAG523D	A	8.5						LAG523E	A	8.8						LAG523F	A	7.9						CLN523A	E	52.1	5.95	4.07	0.69	0.50	0.446	A	8.4	8.58	8.16	CLN523B	E	52.1	6.76	4.78	0.72	0.53	0.490	A	8.4	9.42	8.98	CLN523C	E	52.1	6.20	4.68	0.65	0.52	0.494	A	8.4	9.48	9.03	CLN523D	E	52.1	6.19	4.24	0.69	0.50	0.468	A	8.4	8.99	8.45	CLN523E	E	52.1	6.47	4.62	0.67	0.50	0.504	A	8.4	9.68	9.23	CLN523F	E	52.1	6.23	4.59	0.66	0.51	0.488	A	8.4	9.38	9.03	CLN523G	E	52.1	6.15	4.41	0.67	0.51	0.476	A	8.4	9.14	8.65																				
CLN524G	F	18.7	7.84	6.89	0.84	0.80	0.174																																																																																																																																																																																												
	A	7.9	9.28	8.64				CLN524H	F	18.7	8.43	7.44	0.91	0.81	0.173	A	7.9	9.25	9.24	CLN524I	F	18.7	8.35	7.43	0.87	0.81	0.179	A	7.9	9.58	9.13	LAG523A	E	52.2						LAG523B	E	52.3						LAG523C	E	51.6						LAG523D	A	8.5						LAG523E	A	8.8						LAG523F	A	7.9						CLN523A	E	52.1	5.95	4.07	0.69	0.50	0.446	A	8.4	8.58	8.16	CLN523B	E	52.1	6.76	4.78	0.72	0.53	0.490	A	8.4	9.42	8.98	CLN523C	E	52.1	6.20	4.68	0.65	0.52	0.494	A	8.4	9.48	9.03	CLN523D	E	52.1	6.19	4.24	0.69	0.50	0.468	A	8.4	8.99	8.45	CLN523E	E	52.1	6.47	4.62	0.67	0.50	0.504	A	8.4	9.68	9.23	CLN523F	E	52.1	6.23	4.59	0.66	0.51	0.488	A	8.4	9.38	9.03	CLN523G	E	52.1	6.15	4.41	0.67	0.51	0.476	A	8.4	9.14	8.65																																
CLN524H	F	18.7	8.43	7.44	0.91	0.81	0.173																																																																																																																																																																																												
	A	7.9	9.25	9.24				CLN524I	F	18.7	8.35	7.43	0.87	0.81	0.179	A	7.9	9.58	9.13	LAG523A	E	52.2						LAG523B	E	52.3						LAG523C	E	51.6						LAG523D	A	8.5						LAG523E	A	8.8						LAG523F	A	7.9						CLN523A	E	52.1	5.95	4.07	0.69	0.50	0.446	A	8.4	8.58	8.16	CLN523B	E	52.1	6.76	4.78	0.72	0.53	0.490	A	8.4	9.42	8.98	CLN523C	E	52.1	6.20	4.68	0.65	0.52	0.494	A	8.4	9.48	9.03	CLN523D	E	52.1	6.19	4.24	0.69	0.50	0.468	A	8.4	8.99	8.45	CLN523E	E	52.1	6.47	4.62	0.67	0.50	0.504	A	8.4	9.68	9.23	CLN523F	E	52.1	6.23	4.59	0.66	0.51	0.488	A	8.4	9.38	9.03	CLN523G	E	52.1	6.15	4.41	0.67	0.51	0.476	A	8.4	9.14	8.65																																												
CLN524I	F	18.7	8.35	7.43	0.87	0.81	0.179																																																																																																																																																																																												
	A	7.9	9.58	9.13				LAG523A	E	52.2						LAG523B	E	52.3						LAG523C	E	51.6						LAG523D	A	8.5						LAG523E	A	8.8						LAG523F	A	7.9						CLN523A	E	52.1	5.95	4.07	0.69	0.50	0.446	A	8.4	8.58	8.16	CLN523B	E	52.1	6.76	4.78	0.72	0.53	0.490	A	8.4	9.42	8.98	CLN523C	E	52.1	6.20	4.68	0.65	0.52	0.494	A	8.4	9.48	9.03	CLN523D	E	52.1	6.19	4.24	0.69	0.50	0.468	A	8.4	8.99	8.45	CLN523E	E	52.1	6.47	4.62	0.67	0.50	0.504	A	8.4	9.68	9.23	CLN523F	E	52.1	6.23	4.59	0.66	0.51	0.488	A	8.4	9.38	9.03	CLN523G	E	52.1	6.15	4.41	0.67	0.51	0.476	A	8.4	9.14	8.65																																																								
LAG523A	E	52.2																																																																																																																																																																																																	
LAG523B	E	52.3																																																																																																																																																																																																	
LAG523C	E	51.6																																																																																																																																																																																																	
LAG523D	A	8.5																																																																																																																																																																																																	
LAG523E	A	8.8																																																																																																																																																																																																	
LAG523F	A	7.9																																																																																																																																																																																																	
CLN523A	E	52.1	5.95	4.07	0.69	0.50	0.446																																																																																																																																																																																												
	A	8.4	8.58	8.16				CLN523B	E	52.1	6.76	4.78	0.72	0.53	0.490	A	8.4	9.42	8.98	CLN523C	E	52.1	6.20	4.68	0.65	0.52	0.494	A	8.4	9.48	9.03	CLN523D	E	52.1	6.19	4.24	0.69	0.50	0.468	A	8.4	8.99	8.45	CLN523E	E	52.1	6.47	4.62	0.67	0.50	0.504	A	8.4	9.68	9.23	CLN523F	E	52.1	6.23	4.59	0.66	0.51	0.488	A	8.4	9.38	9.03	CLN523G	E	52.1	6.15	4.41	0.67	0.51	0.476	A	8.4	9.14	8.65																																																																																																																				
CLN523B	E	52.1	6.76	4.78	0.72	0.53	0.490																																																																																																																																																																																												
	A	8.4	9.42	8.98				CLN523C	E	52.1	6.20	4.68	0.65	0.52	0.494	A	8.4	9.48	9.03	CLN523D	E	52.1	6.19	4.24	0.69	0.50	0.468	A	8.4	8.99	8.45	CLN523E	E	52.1	6.47	4.62	0.67	0.50	0.504	A	8.4	9.68	9.23	CLN523F	E	52.1	6.23	4.59	0.66	0.51	0.488	A	8.4	9.38	9.03	CLN523G	E	52.1	6.15	4.41	0.67	0.51	0.476	A	8.4	9.14	8.65																																																																																																																																
CLN523C	E	52.1	6.20	4.68	0.65	0.52	0.494																																																																																																																																																																																												
	A	8.4	9.48	9.03				CLN523D	E	52.1	6.19	4.24	0.69	0.50	0.468	A	8.4	8.99	8.45	CLN523E	E	52.1	6.47	4.62	0.67	0.50	0.504	A	8.4	9.68	9.23	CLN523F	E	52.1	6.23	4.59	0.66	0.51	0.488	A	8.4	9.38	9.03	CLN523G	E	52.1	6.15	4.41	0.67	0.51	0.476	A	8.4	9.14	8.65																																																																																																																																												
CLN523D	E	52.1	6.19	4.24	0.69	0.50	0.468																																																																																																																																																																																												
	A	8.4	8.99	8.45				CLN523E	E	52.1	6.47	4.62	0.67	0.50	0.504	A	8.4	9.68	9.23	CLN523F	E	52.1	6.23	4.59	0.66	0.51	0.488	A	8.4	9.38	9.03	CLN523G	E	52.1	6.15	4.41	0.67	0.51	0.476	A	8.4	9.14	8.65																																																																																																																																																								
CLN523E	E	52.1	6.47	4.62	0.67	0.50	0.504																																																																																																																																																																																												
	A	8.4	9.68	9.23				CLN523F	E	52.1	6.23	4.59	0.66	0.51	0.488	A	8.4	9.38	9.03	CLN523G	E	52.1	6.15	4.41	0.67	0.51	0.476	A	8.4	9.14	8.65																																																																																																																																																																				
CLN523F	E	52.1	6.23	4.59	0.66	0.51	0.488																																																																																																																																																																																												
	A	8.4	9.38	9.03				CLN523G	E	52.1	6.15	4.41	0.67	0.51	0.476	A	8.4	9.14	8.65																																																																																																																																																																																
CLN523G	E	52.1	6.15	4.41	0.67	0.51	0.476																																																																																																																																																																																												
	A	8.4	9.14	8.65																																																																																																																																																																																															

Table 1. Summary of Experimental Results (continued)

Test	Membrane Type	τ (sec)	$K_L a^+$ (*10 ³) (sec ⁻¹)	$K_L a^{++}$ (*10 ³) (sec ⁻¹)	Ratios		Product ($\tau K_L a_T$)
					$\frac{K_L a^+}{K_L a_T}$	$\frac{K_L a^{++}}{K_L a_T}$	
CLN523H	E	52.1	6.65	4.93	0.69	0.53	0.502
	A	8.4	9.65	9.35			
CLN523I	E	52.1	6.55	4.78	0.68	0.52	0.498
	A	8.4	9.58	9.20			
LAG521A	D	10.1					
LAG521B	D	11.0					
LAG521C	D	10.7					
LAG521D	C						
LAG521E	C	5.3					
LAG521F	C	5.2					
CLN521A	D	10.6	8.10	6.95			
	C	5.2	8.71	7.70			
CLN521B	D	10.6	8.54	7.18			
	C	5.2	9.21	7.89			
CLN521C	D	10.6	8.47	6.61			
	C	5.2	8.90	7.19			
CLN521D	D	10.6	8.41	8.02			
	C	5.2	9.07	8.64			
CLN521E	D	10.6	8.93	6.52			
	C	5.2	9.22	7.03			
CLN521F	D	10.6	9.42	8.85			
	C	5.2	9.82	9.47			
LAG514A	B	26.9					
LAG514B	B	26.1					
LAG514C	B	28.9					
LAG514D	A	7.9					
LAG514E	A	7.8					
CLN514A	B	27.3	7.89	6.63	0.88	0.77	0.245
	A	7.8	8.96	8.64			
CLN514B	B	27.3	7.77	6.55	0.86	0.76	0.246
	A	7.8	8.99	8.64			

Table 1. Summary of Experimental Results (continued)

Test	Membrane Type	τ (sec)	$K_L a^+$ (*10 ³) (sec ⁻¹)	$K_L a^{++}$ (*10 ³) (sec ⁻¹)	Ratios		Product ($\tau K_L a_T$)
					$\frac{K_L a^+}{K_L a_T}$	$\frac{K_L a^{++}}{K_L a_T}$	
CLN514C	B	27.3	7.97	6.69	0.87	0.76	0.252
	A	7.8	9.21	8.86			
CLN514D	B	27.3	7.85	6.62	0.86	0.76	0.248
	A	7.8	9.08	8.75			
CLN514E	B	27.3	8.01	6.72	0.88	0.76	0.249
	A	7.8	9.13	8.79			
CLN512A	C	5.4		7.49			
	A	7.8		6.69			
CLN512B	C	5.4		8.05			
	A	7.8		7.39			
CLN512C	C	5.4		6.45			
	A	7.8		5.89			
CLN512D	C	5.4		7.60			
	A	7.8		6.99			
CLN512E	C	5.4		7.53			
	A	7.8		6.89			
LAG511A	C	5.4					
LAG511B	C	4.9					
LAG511C	C	4.8					
LAG511D	C	6.1					
LAG511E	C	5.7					
CLN511	C	5.4	3.75				
	A	7.8	3.69				
LAG505A	A	8.5					
LAG505B	A	8.0					
LAG505C	A	8.5					
LAG505D	A	6.4					
LAG505E	A	7.9					
LAG505F	A	7.1					
CLN505	A	7.7	9.04				
CLN505	A	7.7	8.77				

Table 1. Summary of Experimental Results (continued)

Test	Membrane Type	τ (sec)	$K_L a^+$ (*10 ³) (sec ⁻¹)	$K_L a^{++}$ (*10 ³) (sec ⁻¹)	Ratios		Product ($\tau K_L a_T$)
					$\frac{K_L a^+}{K_L a_T}$	$\frac{K_L a^{++}}{K_L a_T}$	
LAG428A	A	7.8					
LAG428B	A	7.7					
LAG428C	A	7.5					
LAG428D	A	7.6					
CLN428	A	7.7					

τ probe time constant, seconds

+

$K_L A$ estimated by ASCE nonlinear least squares procedure with truncation, seconds

++

$K_L A$ estimated by ASCE nonlinear least squares procedure without truncation, seconds

A 1 standard membrane

B 2 standard membranes

C 1 sensitive membrane

D 2 sensitive membranes

E 3 standard membranes

F 1 sensitive mounts outside of our standard

Table 2. Simulation Results

$K_L a_T$ (*10 ³) (sec ⁻¹)	τ (sec ⁻¹)	$K_L a^+$ (*10 ³) (sec ⁻¹)	$K_L a^{++}$ (*10 ³) (sec ⁻¹)	Ratios		Product ($\tau K_L a_T$)
				$\frac{K_L a^+}{K_L a_T}$	$\frac{K_L a^{++}}{K_L a_T}$	
0.001	5.4	1.00	1.00			
	7.7	1.00	1.00	1.00	1.00	0.008
	10.6	1.00	1.00	1.00	1.00	0.011
	18.7	1.00	0.99	1.00	1.00	0.019
	27.3	1.00	0.99	1.00	0.99	0.027
	31.0	1.00	0.99	1.00	0.99	0.031
	52.0	0.99	0.98	0.99	0.98	0.052
	0.002	5.4	2.00	1.99		
7.7		2.00	1.99	1.00	1.00	0.015
10.6		2.00	1.99	1.00	1.00	0.021
18.7		2.00	1.97	1.00	0.99	0.037
27.3		1.99	1.95	1.00	0.98	0.055
31.0		2.00	1.94	1.00	0.97	0.062
52.0		1.98	1.86	0.99	0.94	0.104
0.004		5.4	4.00	3.97		
	7.7	4.00	3.95	1.00	1.00	0.031
	10.6	4.00	3.93	1.00	0.99	0.042
	18.7	3.99	3.83	1.00	0.97	0.075
	27.3	3.96	3.71	0.99	0.94	0.109
	31.0	3.93	3.65	0.98	0.92	0.124
	52.0	3.70	3.30	0.93	0.83	0.208
	0.005	5.4	5.00	4.95		
7.7		5.00	4.92	1.00	1.00	0.039
10.6		5.00	4.87	1.00	0.99	0.053
18.7		4.97	4.71	0.99	0.96	0.094
27.3		4.88	4.50	0.98	0.91	0.137
31.0		4.83	4.40	0.97	0.89	0.155
52.0		4.40	3.86	0.88	0.78	0.260

Table 2

K_{LaT} (*10 ³) (sec ⁻¹)	τ (sec ⁻¹)	K_{La}^+ (*10 ³) (sec ⁻¹)	K_{La}^{++} (*10 ³) (sec ⁻¹)	Ratios		Product (τK_{LaT})
				$\frac{K_{La}^+}{K_{LaT}}$	$\frac{K_{La}^{++}}{K_{LaT}}$	
0.008	5.4	8.00	7.85			
	7.7	7.99	7.75	1.00	1.00	0.062
	10.6	7.97	7.59	1.00	0.98	0.085
	18.7	7.75	7.09	0.97	0.91	0.150
	27.3	7.33	6.51	0.92	0.84	0.218
	31.0	7.12	6.27	0.89	0.81	0.248
	52.0	5.88	5.01	0.74	0.65	0.416
0.01	5.4	10.00	9.74			
	7.7	9.97	9.56	1.00	1.00	0.077
	10.6	9.90	9.29	0.99	0.97	0.106
	18.7	9.42	8.47	0.94	0.89	0.187
	27.3	8.67	7.58	0.87	0.79	0.273
	31.0	8.32	7.22	0.83	0.75	0.310
	52.0	6.47	5.45	0.65	0.57	0.520

Notes:

 τ probe time constant, seconds+ K_{La} estimated by ASCE nonlinear least squares procedure with truncation, seconds++ K_{La} estimated by ASCE nonlinear least squares procedure without truncation, seconds K_{LaT} True K_{La}

Ratio of Estimated K_La 's to True K_La 's

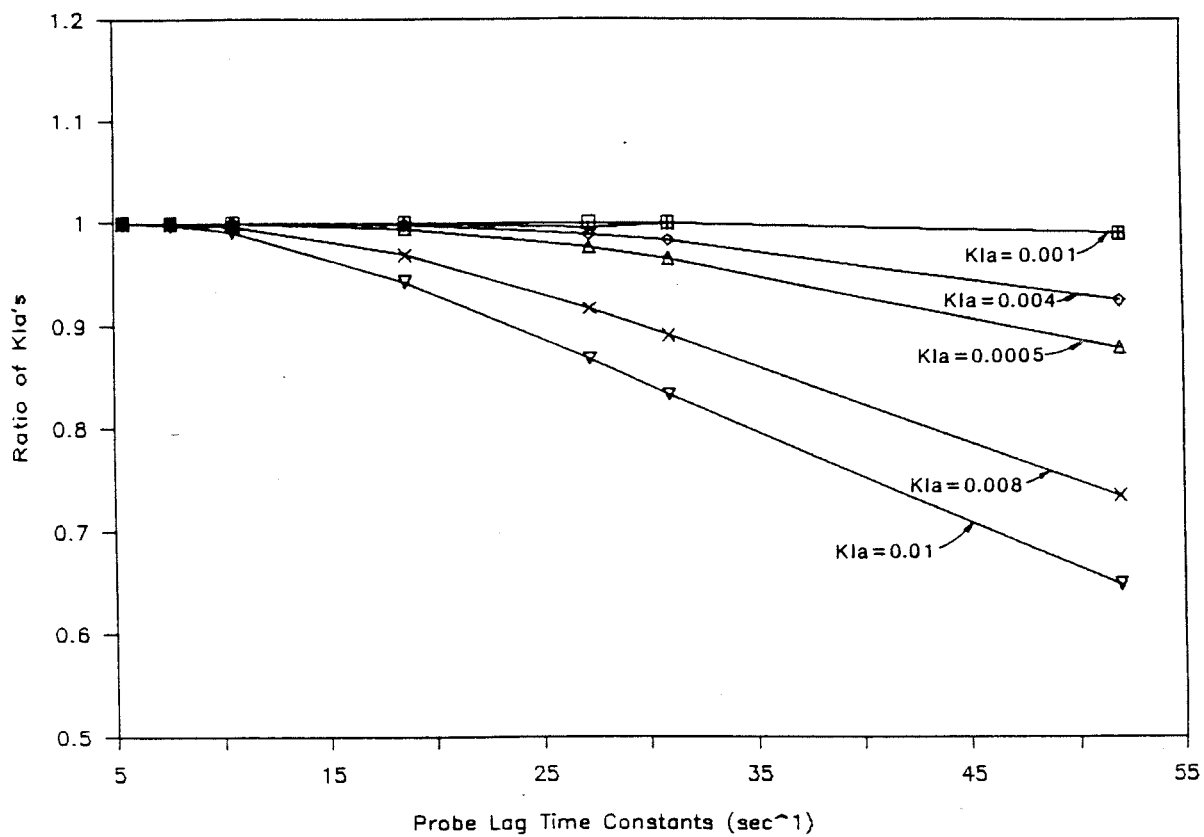


Figure 17. Ratio of Estimated K_La 's to True K_La 's

Ratio of Estimated $K_L a$ to True $K_L a$
for various time probe time constants

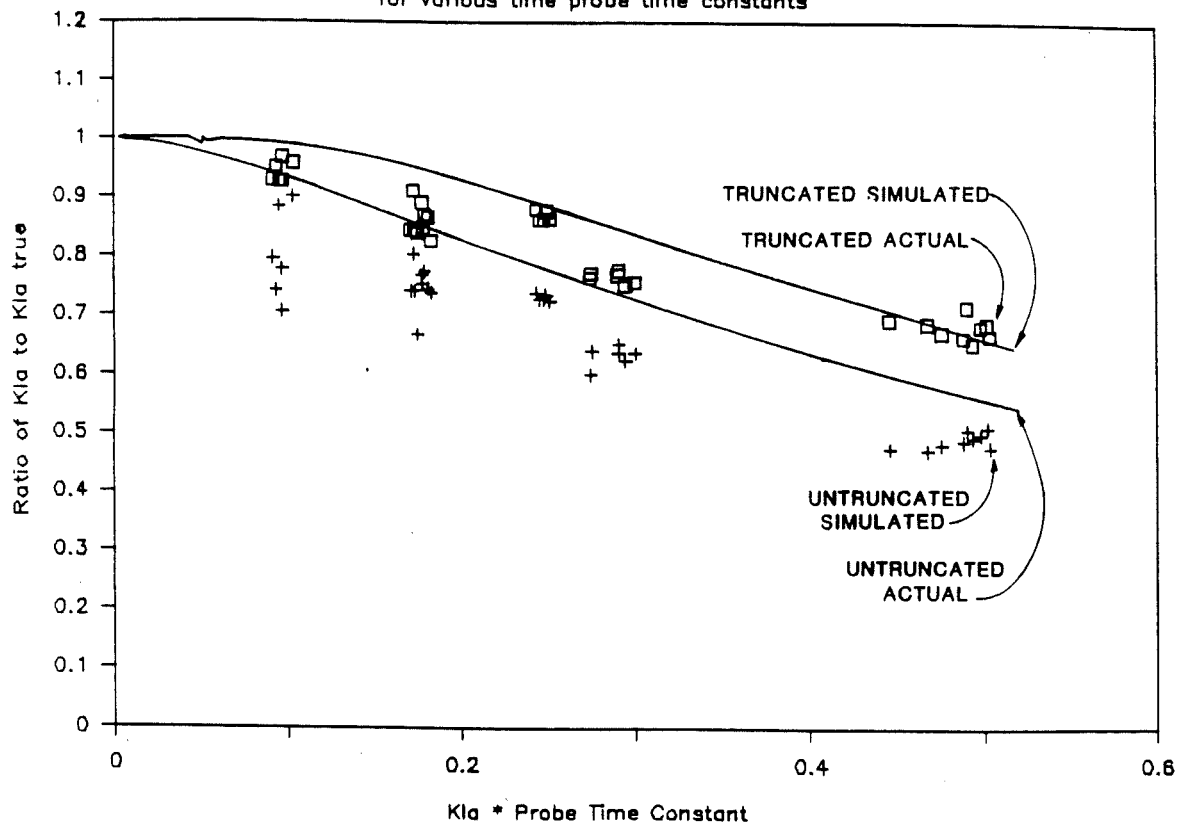


Figure 18. Ratio of Estimated $K_L a$ to True $K_L a$

the truncated and nontruncated data. It should be noted that the data obtained from the 521 tests are included with this plot. A standard membrane was not used in this test; consequently the comparison is not completely justified. Through our simulated data, however, we have verified that this deviation should effect this particular result by less than 0.1%.

For $K_L a$'s calculated from truncated data with $K_L a t$ less than 0.05, there appears to be no discernible error. For very large values of $K_L a t$ then error becomes quite large approaching 40% when $K_L a t$ is greater than 0.5. The ASCE Standard (1984) suggests that the maximum value of $K_L a t$ be 0.02 or less. This suggestion is conversative for results calculated from truncated data, and introduces no discernible error. For results calculated from untruncated data, there is approximately 1% error when $K_L a t$ is 0.02. Truncation improves the parameter estimation procedure, and allows slower probes to be used, as greater values of $K_L a$ are measured.

Figures 19 and 20 show the effects of probe-lag induced error on the "fit" between the DO concentration versus time data and the exponential form of the two film model. Figure 20 shows the residuals for a medium response probe. The untruncated data fits the exponential form very poorly, showing biased residuals with trends. The effect of truncation, which is also shown in Figure 20, reduces the magnitude of the residuals considerably.

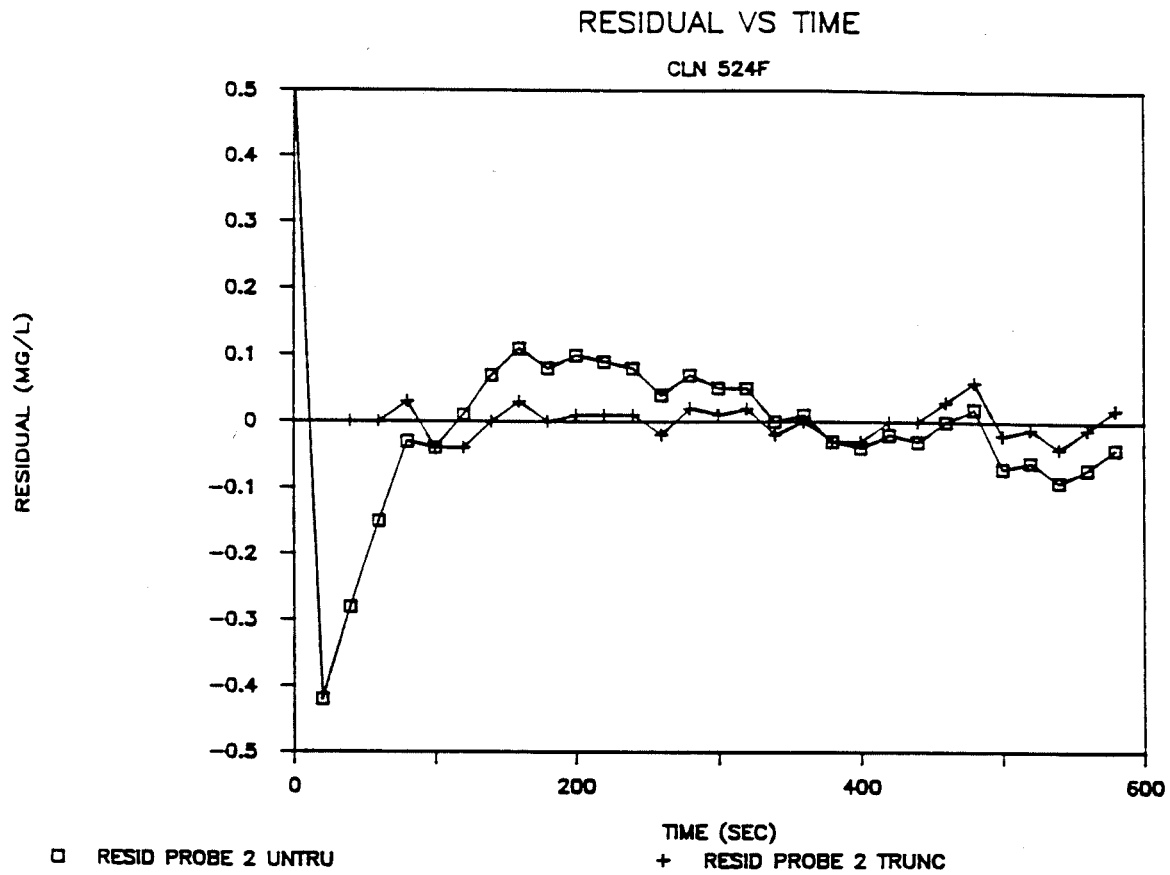


Figure 19. Residuals for a Fast Response Probe Versus Time, Truncated and Untruncated

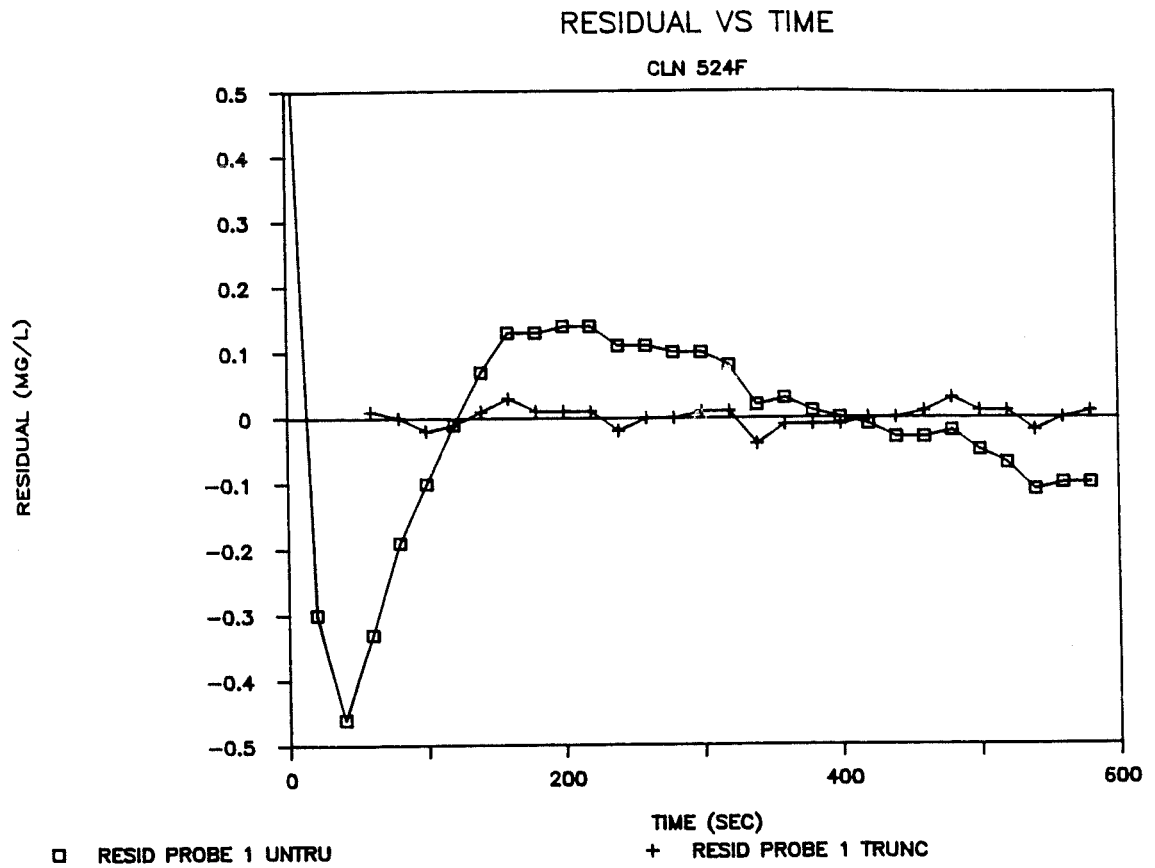


Figure 20. Residuals for a Medium Response Probe Versus Time, Truncated and Untruncated

V. CONCLUSIONS

1. A first-order lag reasonably approximates a polarographic dissolved oxygen probe. The first-order lag more accurately approximates a slowly responding probe. A quickly responding probe appears to behave nonlinearly, and a first-order lag approximation is less accurate. The lag more accurately approximates the probe's response as the dissolved oxygen approaches a higher concentration from a lower concentration.
2. For the probes tested (YSI, 1977) the average lag was 5 seconds for a high-sensitivity membrane, and 7.7 seconds for a standard membrane. The values are probably typical of these types of probes; however, no effort was made to perform comprehensive tests to determine representative lags for the YSI probes.
3. The effects of probe lag on $K_L a$ estimation can be very significant, approaching 40% for the worst conditions tested in this research. To control the magnitude of probe lag induced error to less than 1%, the magnitude of $K_L a \tau$ (dimensionless) should be less than 0.05 if the dissolved oxygen versus time data is truncated at 20%, or 0.02 if no truncation is used. Data truncation at 20% is allowed by the ASCE (1984) Standard, and is recommended to reduce probe-lag induced error.

4. The effects of probe lag can be detected by observing the residuals calculated in the nonlinear ASCE parameter estimation procedure.

VI. REFERENCES

1. American Society of Civil Engineers (1984), *ASCE Standard for the Measurement of Oxygen Transfer in Clean Water*, ASCE, New York.
2. APHA, AWWA & WPCF (1985), *Standard Methods for the Examination of Water and Wastewater*, 16th Edition, Washington, D.C.
3. Aiba, S., Humphrey, A. and Millis, N.F. (1973), *Biomedical Engineering*, 2nd Edition, Academic Press, Inc., New York.
4. Aiba, S. and Huang, S.Y. (1969), "Oxygen Permeability and Diffusivity in Polymer Membranes Immersed in Liquids," *Chemical Engineering Science*, Vol. 24, pp. 1149-1155.
5. Barnes, J.D. (1979), "The Influence of Polymer Membrane Properties on the Performance of Dissolved Oxygen Sensors," National Measurement Laboratory, National Bureau of Standards, NBSIR-79-1740.
6. Boyle, W.C., Berthouex, P.M. and Rooney, T.C. (1974), "Pitfalls in Parameter Estimation for Oxygen Transfer Data," *Journal of the Environmental Engineering Division*, ASCE, pp. 391-408.
7. Brown, L.C. and Baillod, C.R. (1982), "Modeling and Interpreting Oxygen Transfer Data," *Journal of the Environmental Engineering Division*, ASCE, pp. 607-627.
8. Campbell, H.J., Ball, R.O. and O'Brian, J.H. (1976), "Aeration Testing and Design - A Critical Review," presented at the 8th Mid Atlantic Industrial Waste Conference, Newark, Delaware.
9. Clark, L.C. (1956), "Monitor and Control of Blood and Tissue Oxygen Transfer Data," *American Society of Artificial Organs Transactions*, pp. 41-65.
10. Ewing, L., Redmon, D.T. and Wren, J.D. (1977), "Experiences in Testing and Data Analysis of Diffused Aeration Equipment," *Proceedings of the 50th Annual Conference of the Water Pollution Control Federation*, Philadelphia, PA.
11. Gilbert, R.G. and Chen, S.J. (1976), "Testing for Oxygen Transfer Efficiency in a Full-Scale Deep Tank," *Proceedings of the 31st Industrial Waste Conference*, Purdue University, Lafayette, Indiana, pp. 291-311.

12. Hitchman, M.L. (1978), *Measurement of Dissolved Oxygen*, John Wiley and Sons, New York.
13. International Business Machines, "Continuous System Modeling Program III (CSMP III) Program by Manual," Program No. 5734-X59 Ontario: IBM, 1972.
14. Lewis, W.K. and Whitman, W.G. (1924), *Principles of Gas Absorption.*, Industrial and Engineering Chemistry, Vol. 16, pp. 1215-1237.
15. Mancy, K.H. and Westgarth, W.C. (1962), "Galvanic Cell Oxygen Analyzer," *Journal of the Water Pollution Control Federation*, Vol. 34, pp. 1037-1051.
16. Mancy, K.H., Okun, D.A. and Reilley, C.N. (1961), "A Galvanic Cell Oxygen Analyzer," *Journal of Electroanalytical Chemistry*, Vol. 4, pp. 65-91.
17. Morgan, P.F. and Bewtra, J.D. (1962), "Determining Oxygen Uptake Rate by the Polarographic Method," *Journal of the Water Pollution Control Federation*, Vol. 4, pp. 363-375.
18. National Oceanographic Instrumentation Center (1972), *Evaluation of Dissolved Oxygen Analyzers*," NOAA 74051643.
19. Rand, M.C. and Heukelekian, H. (1951), "Determination of Dissolved Oxygen in Industrial Wastes by the Winkler and Polarographic Methods," *Journal of Sewage and Industrial Wastes*, Vol. 23, pp. 1141-1149.
20. Reynolds, J.F. (1969), "Comparison Studies of Winkler versus Oxygen Sensor," *Journal of the Water Pollution Control Federation*, Vol. 41, pp. 2002-2009.
21. Snoeyink, V.L. and Jenkins, D. (1980), *Water Chemistry*, John Wiley and Sons, Inc., New York.
22. Stenstrom, M.K., Vazirinejad, H.R. and Ng, A.S. (1984), "Economic Evaluation of Upgrading Aerations Systems," *Journal of the Water Pollution Control Federation*, Vol. 45, pp. 20-26.
23. Stenstrom, M.K. (1978), "Models for Oxygen Transfer: Their Theoretical Basis and Implications for Industrial Wastewater Treatment," Proceedings of the 33rd Annual Purdue Industrial Waste Conference,

Purdue University, Lafayette, Indiana.

24. *YSI Instruction Manual for YSI Model 57.* Yellow Springs Instrument Co., Yellow Springs, OHIO.